Schwedes + Schulze Schüttguttechnik GmbH

VT-Toolbox

Version 2.0.2

Programmes for calculating process engineering parameters and pneumatic conveying systems.

© 2025-2030 Mario Dikty

Content

	P	age
1	Licence	4
2	Before you start	6 7
3	Basics of pneumatic conveying 3.1 Introduction	9101213151721
4	Inhalt der VT - Toolbox	23
5	Using the Toolbox (Pneumatic conveying)	24
	 5.2.1 Limits of use of the programme 5.2.2 Entering the bulk solids data 5.2.3 Entering the plant / system data 5.2.4 Calculation results 5.3 Overpressure conveying based on the drag coefficient by Siegel [3] 5.3.1 Einsatzgrenzen des Programmes 5.3.2 Input of the bulk solid data 5.4 Vacuum conveying based on the drag coefficients by Siegel [3] 5.4.1 Limits of the program module 5.4.2 Bulk solid input data 5.5 Overpressure conveying based on the calculation of Stegmaier's drag coefficient for fine bulk solids (ds,50 ≤ 150 μm) 5.5.1 Limits of the program module 5.5.2 Input of the bulk solid data 5.5.3 Intermediate calculations 	27 27 28 29 31 31 36 36 36
	5.6 Vacuum conveying based on the calculation of the Stegmaier drag coefficient for fine bulk solids ($d_{s.50} \le 150 \mu m$)	39

	5.6.1 Limits of the program module3	39
	5.7 Evaluation of the results	
	5.8 Remarks on the design of blowers and compressors4	
6	Operating the VT - Toolbox (Additional Modules)4	12.
Ŭ	6.1 Calculation of the thermal expansion of pipework4	
	6.2 Velocities in pipes4	
	6.3 Conversion of velocites and volume flows depending on the pressure and	
	temperature4	
	6.3.1 Standard- vs. Operational Conditions4	
	6.3.2 Gas equation4	
	6.3.3 Plant altitude4	
	6.4 Single particle settling velocity4	
	6.5 Fluidizing / Loosening velocity4	
	6.6 Rotary valve dimensioning acc. ISO 39224	17
	6.7 Pressure loss of air pipes acc. VDI-Wärmeatlas	
	6.7.1 Pressure loss of a "10 m section"5	
	6.7.2 Pressure loss of a 90° bend	
	6.8 Geldart-Diagram (in progress)5	
	sio Gordan Diagram (in progress)	_
7	List of symbols5	55
8	Literature	57

1 Licence

Read this licence carefully before using this product. By using this product, you acknowledge that you have read this licence and agree to its terms and conditions.

Licence conditions

Schwedes + Schulze Schüttguttechnik GmbH ("we" or "us") provides you with media comprising a computer program (the "Program"), the licence (the "Licence") and user manual (together the "Product") and grants you the right to use the Product in accordance with the terms of this Licence. The copyright and all other rights to this Product remain with us.

The programme is only available as a web version.

You may not:

- 1. use or make copies of this product other than as described in the licence or make copies of it;
- 2. reverse compile, decompile or disassemble the program, unless this restriction is prohibited by applicable law; modify the program or combine any or all parts of the program with other programs.
- 3. disclose your access data to third parties.

Validity

This licence is valid for as long as you use the product. However, the licence ends as soon as you violate any of the conditions listed here. The limitations of warranty and liability set out below shall survive the expiry of the licence.

Warranty and limitation of liability

The product is provided on an "as is" basis, without any other warranties, express or implied, including those of fitness for a particular purpose, or those based on statute, regulation or custom. The entire risk as to the results and operation of the product is assumed by you. We will not be liable to you or any other person or organisation for any indirect, consequential or incidental damages, including, but not limited to, loss of revenue or profit, lost or corrupted data or other commercial or economic loss, even if we have been advised of the possibility of such damages or they were foreseeable; or for claims by third parties. The amount of our liability to you is limited to the amount paid by you for the product. We accept no liability for incorrect operation of the programme.

User qualification

The programme must be used with process engineering expertise. The programme may only be used by process engineers. If employees without process engineering training use the programme, this can lead to serious misinterpretations. This incorrect operation cannot be ruled out by the programme. In addition, we recommend attending the Schwedes + Schulze GmbH training course on "Pneumatic conveying" to gain an insight into the basics of the VT-Toolbox. In this training course, the design approaches used in the VT-Toolbox are presented.

General Information

This Licence is the entire agreement between us, supersedes any other agreement or understanding, oral or written, and is not modified except by a written and signed agreement. This Licence shall be governed by and construed in accordance with the laws of the Federal Republic of Germany. If any provision of this Licence is held by a court of competent jurisdiction to be illegal, unenforceable or invalid, that provision shall be severed from this Licence and the other provisions shall remain in full force and effect.

Copyright

© 2025-2030 Mario Dikty

The contents of this manual and the associated computer programme "S+S Toolbox-V.N.N.N" are the property of Schwedes + Schulze Schüttguttechnik GmbH and are protected by copyright. Any reproduction in whole or in part is prohibited.

Questions

If you have any problems using the programme, please address your questions to:

Schwedes + Schulze Schüttguttechnik GmbH Teichstrasse 4 21641 Apensen

E-mail: m.dikty@schwedes-und-schulze.de

2 Before you start...

It is assumed that the user is familiar with the basics of pneumatic conveying and process engineering in general. This means that the user is capable of using the programme in the correct manner and interpreting the results carefully and critically. Input errors are not automatically recognised and eliminated by the program. Incorrect inputs lead to incorrect results or, in the worst case, to a programme abort with loss of data. The user is responsible for every calculation result.

2.1 Input cells

The input cells are not locked. All unlocked cells must be filled with input data so that a calculation can be carried out. All other cells are locked in order to avoid accidental overwriting of the calculation smoothing.

Cells with a white or background are input cells.

Cells with a grey background are "result cells". They show the relevant calculation results. They are calculated automatically by using the calculation button.

Figure 1 shows an example of the cell types.

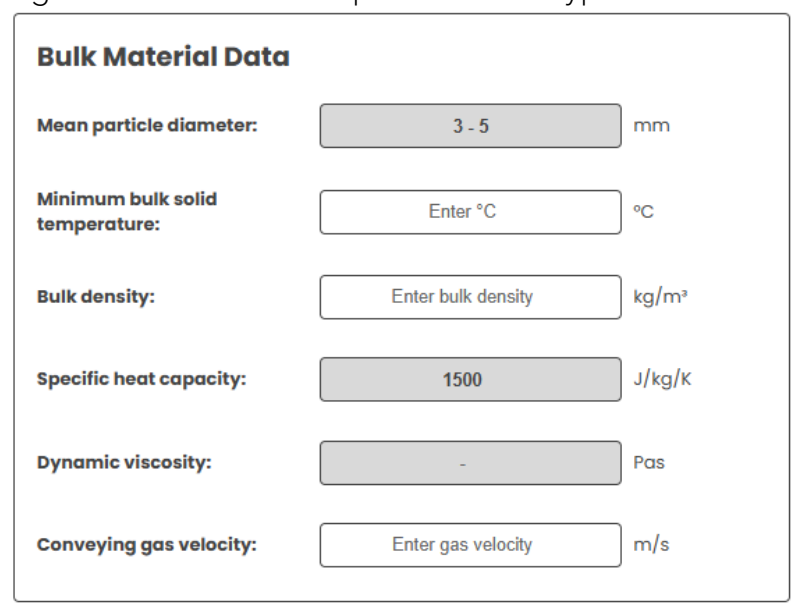


Bild 1: Example of cell colours

2.2 Units

As a rule, the input data must be entered in SI units. Some values, such as particle sizes, are entered partially in [mm], or mass flows in [kg/h]. The user recognises the required unit of the input value from the respective cell next to the input cell. Figure 2 shows the input cells of bulk material parameters. The "average particle diameter" must be entered here in [mm].

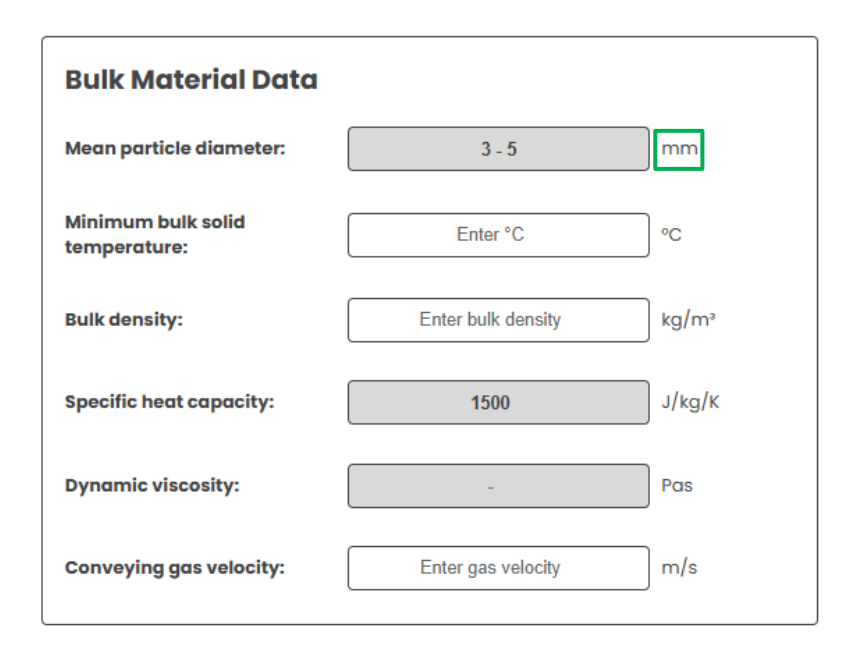


Bild 2: Example Input data with units

2.3 Navigation

The "Back to selection" field provides an overview of the programmes / modules. Clicking on the grey buttons (Fig. 3) takes the user to the respective programme.

$\leftarrow \textbf{Back to Selection}$

Bild 3: Button "Back to selection"

There are at least two additional buttons on each page (Fig. 4). One of them carries out the calculation after the input results have been entered ("Calculate").

Please note: If you have purchased a licence that only allows you to perform a limited number of calculations, the number of calculations you can still perform will be deducted each time you start a calculation.

The execution of calculations from the additional modules (everything except for pneumatic calculations) is free during the licence period. You can carry out as many calculations as you wish.

The second button prints the calculation result or the content of the respective page as a PDF. The file name, which can be freely renamed, is specified by the programme. The file name is made up of the name of the tab and the current date.

Calculate Download PDF

Bild 4: Buttons "Calculate" and "Download PDF"

3 Basics of pneumatic conveying

3.1 Introduction

Technically, pneumatic transport is used in a variety of applications to transport bulk materials through a pipeline, usually in a circular design, by means of a conveying gas, usually air. This takes place either in suction or pressure mode. Figure 5 shows the schematic structure of both systems. Both systems are characterised by a negative pressure gradient in the direction of flow. The basic operations of a suction or pressure system are identical:

- Injection of the bulk material into the conveying line.
- Transport through the conveying line due to a negative pressure difference.
- Separation of the bulk material from the conveying gas at the receiving point (exceptions are, for example, direct reactor or burner feeds for pressurised conveying, such as coal firing in the power plant or cement industry)
- Pressure generation (overpressure for pressure conveying, underpressure for vacuum conveying).

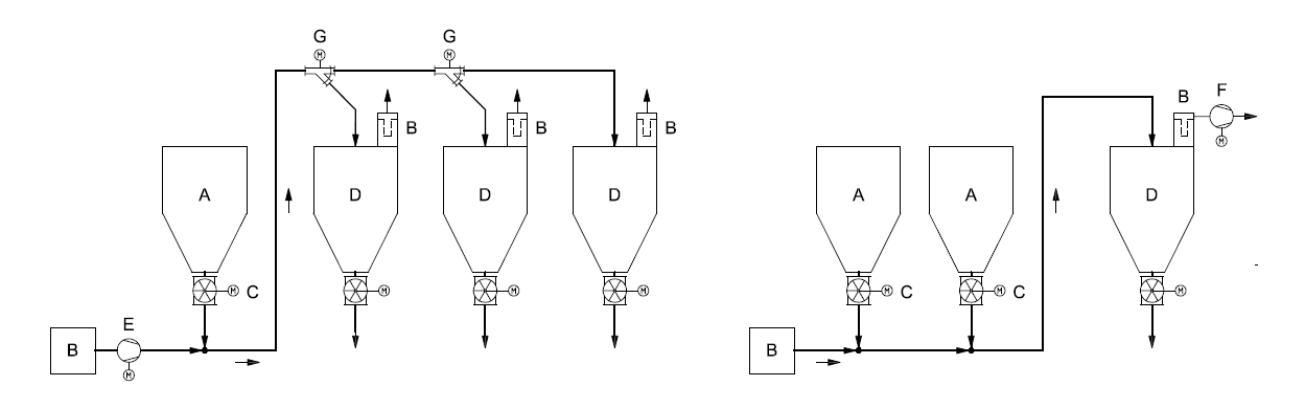


Bild 5: Pressure system (left) / vacuum system (right) based on [1] with "A" storage silo, "B" filter, "C" airlock, "D" receiving silo, "E" overpressure generator, "F" vacuum generator, "G" conveying line diverters

The feeding of the bulk solid into the conveying line in pressurised operation by means of a rotary valve, pressure vessel, screw pump, injector (nozzle conveyor), flap systems or, in the case of exclusively vertical transport, by means of an airlift. At the receiving point, the bulk material is separated from the transport gas for further processing. This is done using cyclones and filters. In burner loading, for example, there is no separation of the 2 phases. The fuel-air mixture is fed directly to the burner lance. The transport gas also serves as combustion air.

The pipe is usually round. Depending on the application, mild steel or, as is common in the chemical and food industries, stainless steel can be used. Wall thicknesses vary from 1 mm to 10 mm.

Compressed air generation depends directly on the feeding system. While pressure vessel systems are equipped with compressors, blowers (up to 1.0 bar(g)) and compressors (up to 2.0 bar(g)) supply screw pumps and rotary valves. Flaps and injectors are almost exclusively combined with blowers. Exceptions to the combinations listed above are possible.

Whether a pneumatic conveying system is used in preference to a mechanical one depends on many criteria. In most cases, the decision is made in favour of pneumatic conveying if the conveying path is either very long or the distance between the starting and receiving points is characterised by deflections and height differences. Other criteria in favour (+) and against (-) pneumatic conveying are [5]:

- High adaptability of the conveyor lines to local conditions (+),
- Environmentally friendly design (no dust emissions) (+),
- Variety of switching options thanks to conveying line diverters (+),
- Low maintenance requirements for the conveying pipe (+),
- Use of inert gas for air-sensitive solids (+),
- Conveying of toxic and hazardous bulk solids (+),
- Wide range of applications for a wide variety of solids (+),
- direct transport into systems that are pressurised (+),
- lower installation costs (+),
- less space required (+),
- realisation of chemical or physical processes during conveying (+),
- comparatively high power requirement (-),
- Wear of pipeline and feeding units (-),
- Can be used economically up to a grain size of approx. 10 mm (-),
- Product abrasion, which may require costly conveying air cleaning (-),
- Risk of dust explosions (-),
- Noise emissions from the pressure generators and the pipework in the case of granulates (-).

3.2 Flow modes

The flow modes describe the flow behaviour of the bulk material in the conveying pipe. It is not always constant throughout the entire system. While, for example, the bulk material still flows through the pipe in the form of dunes (see definition below) at the beginning of the conveying pipe, it can leave the conveying pipe at the end, depending on the system configuration, as a dilute flow (see definition below). The definition of flow mods in horizontal conveying used in this review is based on Weber [6] and Klinzing et al [7] and is shown graphically in Figure 6:

- Mode A: Dilute flow: No occurrence of strands or deposits. This type of flow is also referred to homogeneous flow.
- Mode B: Clusters / small dunes slide on the pipe bottom. Particles flow between the clusters at a higher velocity.
- Mode C: Strand flow: A strand (almost flat surface) that moves or lies motionless on the bottom of the pipe.
- Mode D: Strand flow / stratified flow: One strand flows over a lower strand. The lower strand may or may not move.
- Mode E: Dune flow: A dune (uneven surface, geometry similar to a sand dune) flows through the pipe. A lower strand (flowing or not) may or may not be present.
- Mode F: Plug flow: Plugs flow through the pipe at low velocity. The geometry is like a sand dune that fills the entire vertical pipe cross-section. The plugs take up bulk material at the front and lose bulk material at the end.

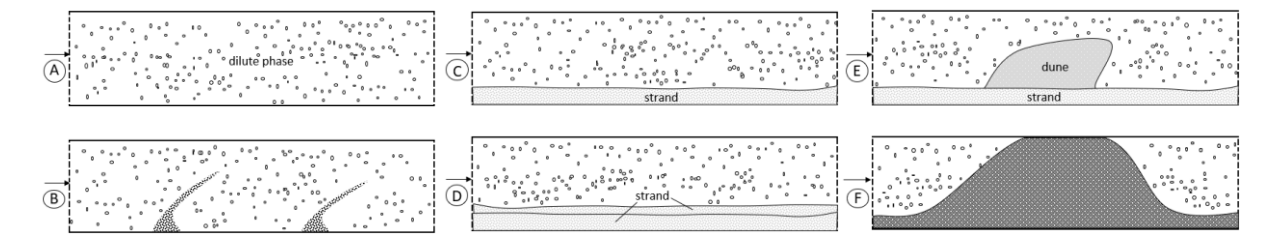


Bild 6: Flow modes of a pneumatic conveying system

High flow velocities prevail during dilute conveying, fine bulk solids ($d_{5,50}$ < 100 µm) behave like coarse bulk solids / granulates. They flow almost evenly across the pipe cross-section.

When the transport gas velocity drops to/below the saltation velocity, the two-phase flow begins to separate, which is referred to as strand conveying. Part of the solid material slides as a strand on the pipe bottom, while the other part is transported over the strand in dilute flow. The strand is essentially driven by impacting particles. Compared to coarse-grained material ($d_{s,50} > 100 \, \mu m$), fine-grained material tends to form strands even at higher air velocities. If the air velocity is reduced further, individual strands can push together to form dunes or plugs. Dunes flow like waves through the conveying line, as shear forces act on the strand surface flowing on the pipe bottom.

Dune flow is an unsteady flow for coarse particles and plug conveying for finegrained bulk solids, where there is a risk of pipe blockages. Closed plugs can form which, if they are longer, block the conveying line due to the wedge effect and the low gas permeability of the bulk material. Under these conveying conditions, safe pneumatic conveying can often only be achieved with additional aids, such as an internal aeration pipe to increase the turbulence in the system. With coarse-grained goods, such wedge effects in the plug are low, so that problem-free conveying can also be achieved here.

3.3 Pressure loss calculation

When dimensioning a pneumatic conveying system, the necessary conveying line pressure loss Δp_{ges} and the required conveying gas volume \dot{V}_F are of the greatest interest. The mass flow rate, pipeline routing and transport medium are generally predetermined by the process and system. This means that only the choice of pipe diameter d_R or, if the pipe diameter is specified, the choice of the desired pressure loss remains for dimensioning. As a result, the pipeline pressure loss and the associated gas volume are obtained.

The total pressure loss Δp_{to} of a conveying line is made up of the pressure loss terms shown in Figures 7 and 8:

- $\Delta p_{F,ges}$ = Pressure loss of transport gas / Fluid
- Δp_{ac} = Pressure loss due to acceleration of the bulk solid
- Δp_{ve} = Vertical pressure loss due to solid friction
- Δp_{fi} = Pressure loss due to fittings in the conveying line (flat, diverter gates)
- Δp_{ho} = Horizontal pressure loss due to solid friction
- Δp_{he} = Pressure loss due to bends

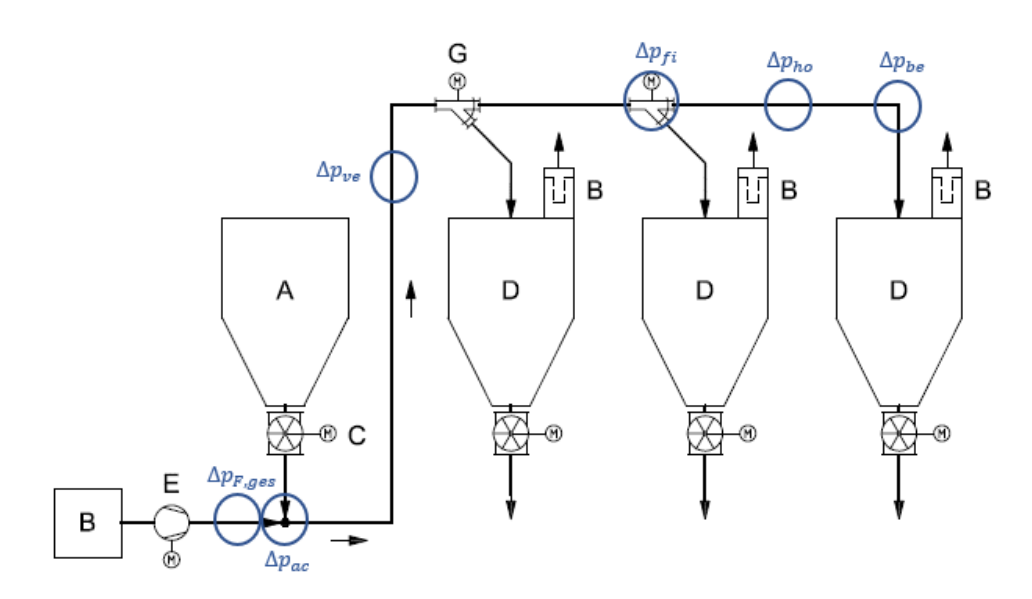


Bild 7: Structure and pressure losses of a pneumatic pressurised conveying system (with A: starting silo, B: filter, C: feed-in device, D: receiving silo, E: pressure generator, G: conveying line diverter)

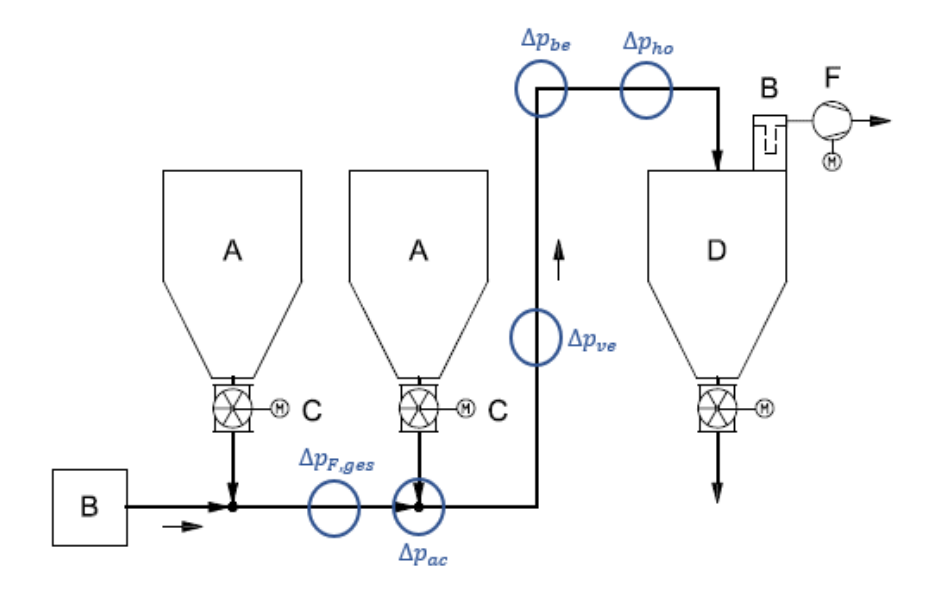


Bild 8: Structure and pressure losses of a pneumatic vacuum conveyor (with A: starting silo, B: filter, C: feed-in device, D: receiving silo, F: vacuum generator)

The total pressure loss results from this:

$$\Delta p_{to} = \Delta p_{F,aes} + \Delta p_{ac} + \Delta p_{ve} + \Delta p_{fi} + \Delta p_{ho} + \Delta p_{be} \tag{1}$$

The pressure loss due to fittings Δp_{fi} depends on the geometry of the fittings. Similar to single-phase flow, there are specific resistance coefficients for internals λ_{fi} , which are also dependent on the bulk material.

$$\Delta p_{fi} = \sum_{k} \lambda_{fi} \cdot \frac{\rho_F}{2} \cdot v_F^2 \tag{2}$$

k represents the sum of the resistances.

Firstly, the pressure loss of the single-phase flow of the gas flow $\Delta p_{F,ges}$ is derived below. The pressure losses of the other terms are then worked out. It is assumed that the gas flow is incompressible and remains unaffected by the simultaneous flow of bulk solids.

3.3.1 Pressure loss oft he gas phase

The pressure loss of the gas phase $\Delta p_{F,ges}$ with the pipe wall is generated via the wall shear stresses. This can be derived using the momentum balance:

$$-\dot{m}_F \cdot dv_F = A_R \cdot dp_F - F_{F,R} \tag{3}$$

The change in momentum flow in the above equation describes the instantaneous acceleration of the mass under consideration. If this term is neglected, an incompressible flow is assumed and the balances may only be solved over short lengths



dL, in which the velocity changes are correspondingly small. This results in the drag force $F_{F,R}$ for the incompressible case:

$$F_{F,R} = A_R \cdot dp_F = \frac{\pi}{4} \cdot d_R^2 \cdot dp_F \tag{4}$$

The resistance force $F_{F,R}$ is caused by the frictional force caused by the wall shear stress $\tau_{F,R}$:

$$F_{F,R} = \tau_{F,R} \cdot A = \tau_{F,R} \cdot \pi \cdot d_R \cdot L_R \tag{5}$$

With the wall shear stress $\tau_{F,R}$:

$$\tau_{F,R} = \lambda_W \cdot \frac{\rho_F}{2} \cdot v_F^2 \tag{6}$$

The pipe drag coefficient λ_F is by definition:

$$\lambda_F = 4 \cdot \lambda_W \tag{7}$$

Now the equations are combined, rearranged and solved:

$$dp_F = \lambda_F \cdot \frac{\rho_F}{2} \cdot v_F^2 \cdot \frac{L_R}{d_R} \tag{8}$$

Since the bulk material occupies part of the balance space, equation (8) must be extended by the volume fraction of the transport gas:

$$-dp_F = \varepsilon_F \cdot \lambda_F \cdot \frac{\rho_F}{2} \cdot v_F^2 \cdot \frac{L_R}{d_P} \tag{9}$$

The pipe friction coefficient λ_F remains as an unknown. Blasius [8] gives Eq. (38) for the drag coefficient for smooth pipes:

$$\lambda_F = 0.0054 + \frac{0.3964}{Re^{0.3}} \tag{10}$$

Eq. (9) can therefore be used to calculate the pressure loss of hydraulically smooth pipes. The validity range of the equation covers the entire range of pneumatic conveying with $2 \cdot 10^4 \le Re \le 2 \cdot 10^6$.

Using the Moody diagram [9] in Figure 9, it is also possible to determine the resistance coefficient as a function of the pipe roughness k_s .

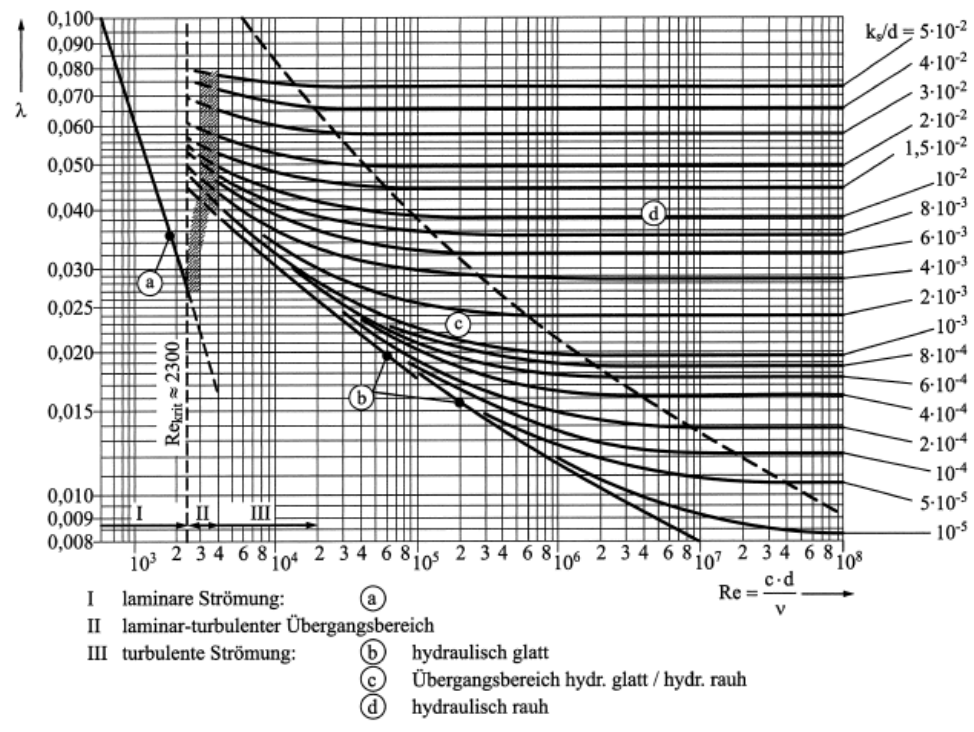


Bild 9: Moody diagram for technically rough straight pipes [9]

When calculating the pressure difference in complex pipelines, in addition to the losses in the straight pipe sections, those resulting from internals, cross-sectional changes and deflections as well as those resulting from gas expansion must also be taken into account. in practice, the drag coefficient λ_{fi} depends solely on the geometry and is largely independent of the Reynolds number in the fully turbulent range. To calculate the total resistance of a pipeline, all partial resistances in a pipe are added together [11]:

$$-\Delta p_{F,ges} = \sum_{i} \left(\varepsilon_{F} \cdot \lambda_{F} \cdot \frac{\rho_{F}}{2} \cdot v_{F}^{2} \cdot \frac{L_{R}}{d_{R}} \right) + \sum_{j} \left(\lambda_{fi} \cdot \frac{\rho_{F}}{2} \cdot v_{F}^{2} \right)$$

$$\tag{11}$$

i represents the sum of the tubular elements, j the sum of the additional resistances.

3.3.2 Pressure loss calculation of the bulk solid acceleration

If the bulk material is fed into the conveying line via the feed device (rotary valve, screw pump, flap, airlift, jetfeeder or pressure vessel), it must be accelerated. As a rule, the starting speed of the bulk material is almost 0, the final acceleration velocity is always less than the conveying gas velocity. The velocity ratio occurring in the stationary state is the so-called slip factor c_{SL} :

$$c_{SL} = \frac{v_S}{v_F} \tag{12}$$

Hilgraf [5] gives the following equations for the slip factor of fine-grained bulk solids:



$$c_{SL} = 1 - \frac{w_{Tr}}{v_F} \tag{13}$$

with:
$$w_{Tr} = 2.28 \cdot \frac{\eta_F}{d_S \cdot \rho_F} \cdot Ar^{0.419}$$
 (14)

and the Archimedes number:

$$Ar = \frac{d_{S,50}^3 \cdot g}{\eta_F^2} \cdot \rho_F \cdot (\rho_P - \rho_F) \tag{15}$$

Further calculation approaches for the slip factor can be found in [16].

The following applies to the acceleration of the bulk solids in one phase:

$$-\dot{m}_S \cdot dv_S = A_R \cdot dp_{ac} \tag{16}$$

The solid loading ratio SLR is introduced for a clearer visualisation of the pressure loss. It represents the ratio of the bulk solids mass flow \dot{m}_S to the conveying gas mass flow \dot{m}_F . The advantage of the SLR μ is that it is independent of pressure and temperature and is constant along the entire conveying section L_R :

$$\mu = \frac{\dot{m}_S}{\dot{m}_F} = \frac{\dot{v}_S \cdot \rho_S}{\dot{v}_F \cdot \rho_F} = \frac{(1 - \varepsilon_F) \cdot v_S \cdot \rho_S \cdot A_R}{\varepsilon_F \cdot v_F \cdot \rho_F \cdot A_R} \tag{17}$$

The change in the true velocity v_s of Eq. (16) is:

$$\Delta v_s = v_{s,in} - v_{s,out} = v_{s,in} - 0 = \frac{v_{s,in}}{v_{F,in}} \cdot v_{F,in} = c_{sL} \cdot v_{F,in}$$
(18)

A combination of equations (16-18) produces the classical representation of the acceleration pressure loss:

$$\Delta p_{ac} \cdot A_R = -\varepsilon_F \cdot c_{SL} \cdot v_F \cdot \mu \cdot v_F \cdot \rho_F \cdot A_R \tag{19}$$

$$\Delta p_{ac} = -\varepsilon_F \cdot c_{SL} \cdot \mu \cdot \rho_F \cdot v_{F,in}^2 \tag{20}$$

Due to the fact that $\varepsilon_F \gg \varepsilon_S$ is $\varepsilon_F \rightarrow 1$ and Eq. (20) can be written as follows, as is usual in the literature:

$$-dp_{ac} = c_s \cdot \mu \cdot \rho_F \cdot v_{F,in}^2 \tag{21}$$

3.3.3 Pressure loss calculation of the solids diverter [5]

Due to the particle inertia and the centrifugal force acting on the particles, the gas phase and the solid phase segregate in a pipe bend. The bulk material is slowed down by the wall friction and must be accelerated again after the bend. The pressure loss generated by a deflection Δp_{be} is therefore the pressure loss required for reacceleration. Equations (16-18) are reused and adapted.

$$-\dot{m}_S \cdot dv_S = A_R \cdot dp_{be} \tag{22}$$

with:
$$\Delta v_s = v_{s,in} - v_{s,out} = \frac{\Delta v_s}{v_{s,in}} \cdot v_{s,in}$$

follows:
$$-\Delta p_{be} = \varepsilon_F \cdot \mu \cdot v_F \cdot \rho_F \cdot (v_{s.out} - v_{s.in})$$
 (23)

Further approaches to pressure loss for bends as well as approaches that take into account the position and orientation of bends can be found in [11, 12, 19 - 24].

3.3.4 Pressure loss calculation of the horizontal bulk solid transport

The pressure loss term of the horizontal flow is derived based on Hilgraf [5]. It leads to a representation that Gasterstädt already presented in 1924 [35] analogue to the calculation approach for the pressure loss of the unloaded pipe flow.

The momentum balance of the multiphase flow can be simplified as follows, assuming incompressible pneumatic conveying in the steady state:

$$-dp_{S,ho} = (1 - \varepsilon_F) \cdot \frac{F_{R,S}}{A_R} \tag{24}$$

The resistance of the solid $F_{S,R}$ is primarily caused by the particle/wall contacts during dilute flow. The resistance coefficient λ_S^* is introduced to visualise the pressure loss; it represents the friction in the form of impact losses between the bulk solid and the pipe wall. The pressure loss for the bulk solids phase can be calculated analogue to equation (9):

$$-dp_{S,ho} = (1 - \varepsilon_F) \cdot \lambda_S^* \cdot \frac{\rho_S}{2} \cdot v_S^2 \cdot \frac{dL_R}{d_R} = \frac{dm_S}{A_R} \cdot \lambda_S^* \cdot \frac{v_S^2}{2 \cdot d_R}$$
 (25)

As the velocity decreases, the bulk material falls out of the gas phase and collects at the pipe bottom, where it is transported as a strand at a slower velocity. If the velocity is so low that no particles flow in the dilute phase, the pressure loss caused by the bulk solids is exclusively due to the sliding friction of the bulk solids on the pipe bottom. The solid resistance is therefore the product of the frictional mass m_S , the weight force g and the coefficient of friction g.

$$F_{ho,S} = dm_S \cdot g \cdot \beta_R = (dV_{S,R} \cdot \rho_P) \cdot g \cdot \beta_R = (dL_R \cdot (1 - \varepsilon_F) \cdot A_{S,R} \cdot \rho_P) \cdot g \cdot \beta_R \tag{26}$$

It should be noted that $A_{S,R}$ is the area of the pipe cross-section covered by the bulk material.



In practice, both flow forms, that of the dilute flow Eq. (25) and that of the pure strand conveying Eq. (26), and thus both resistances overlap. Eq. (25) and Eq. (26) can therefore be combined. For better usability of the resulting equation, the bulk material mass m_S is replaced as follows:

$$dm_S = \dot{m}_S \cdot dt = \frac{\dot{m}_S \cdot dL_R}{v_S} \tag{27}$$

It follows:

$$-dp_{ho,S} = \frac{\dot{m}_S \cdot dL_R}{v_S \cdot A_R} \cdot \left(\lambda_S^* \frac{v_S^2}{2 \cdot d_R} + g \cdot \beta_R\right) \tag{28}$$

The usual form of representation of the horizontal bulk solids pressure loss $dp_{ho,S}$ is obtained when the loading μ , the slip factor c_{SL} and the pipe Froude number Fr_R are used in (28). The Froude number Fr_R is defined as:

$$Fr_R = \frac{v_F^2}{g \cdot d_R} \tag{29}$$

It follows:

$$-dp_{ho,S} = \varepsilon_F \cdot \mu \cdot \lambda_S \cdot \frac{dL_R}{d_R} \cdot \frac{\rho_F}{2} \cdot v_F^2 \tag{30}$$

with the total drag coefficient λ_s according to [43]:

$$\lambda_S = c_{SL} \cdot \lambda_S^* + \frac{2 \cdot \beta_R}{c_{SL} \cdot Fr_R} \tag{31}$$

The friction coefficient β_R can assume the following values [5]:

Dilute flow: $\beta_R = \frac{w_S}{v_F}$, with the terminal velocity w_S

Strand flow: $\beta_R = \tan \varphi_W$, with the wall friction angle φ_W

Plug conveying: $\beta_R = \kappa \cdot \tan \varphi_{W}$, with $\kappa > 1$ as amplification factor, caused

by wedging of bulk material

Eq. (25) predominates in the area of dilute flow:

 $(c_{SL} \cdot \lambda_S^*) \gg \frac{2 \cdot \beta_R}{c_{SL} \cdot Fr_R}$, it follows $\lambda_S \cong const.$ The pressure loss is therefore proportional to the mass inertia force.

Eq. (26) predominates in the area of dense phase conveying:

 $\frac{2 \cdot \beta_R}{c_{SL} \cdot Fr_R} \gg (c_{SL} \cdot \lambda_S^*)$, it follows $\lambda_S \cong \frac{1}{Fr_R}$. The pressure loss is therefore proportional to the weight force.

In addition to the approach for calculating the horizontal pressure loss $dp_{ho,S}$ derived from the force balance, there are other, mostly bulk solids-specific empirical approaches for determining the horizontal pressure loss term [16, 17, 25 - 31], whereby these are generally based on a corresponding λ_S value.



The λ_S is influenced by a large number of bulk solids and system-specific parameters. Empirical approaches take into account the loading μ , the particle diameter $d_{S,50}$ and the Froude number Fr. The particle size distribution: the pairing of wall material / bulk solids or the particle shape are generally not taken into account. Values available in the literature [11, 13, 14, 15, 18, 19] are specific to bulk solids and are not generally applicable. [10] gives the following equation for the λ_S for fine-grained bulk solids $(d_{S,50} < 150 \ \mu m)$:

$$\lambda_{S} = 2.1 \cdot \frac{Fr_{P}^{0.25}}{Fr_{R}} \cdot \frac{1}{\mu^{0.3}} \cdot \left(\frac{d_{R}}{d_{S.50}}\right)^{0.1}$$
(32)

The Froude numbers used by Stegmaier [26] must be considered carefully. The particle Froude number Fr_P , and the pipe Froude number Fr_R are used. The characterising diameter of the particle Froude number is the mean particle diameter $d_{S,50}$. The associated velocity is the settling velocity of the individual particles. It should be noted that the scatter of the measured values around the equalisation line is very high [33]. Figure 10 shows the measurement results published by Stegmaier and their position in the measurement value field. Conveying tests in test systems are necessary to determine the exact resistance value. The equation (32) provided by Stegmaier for the resistance coefficient is an equation with a high degree of scatter. If this calculation approach is used, sufficient allowances must be taken into account in the calculation results.

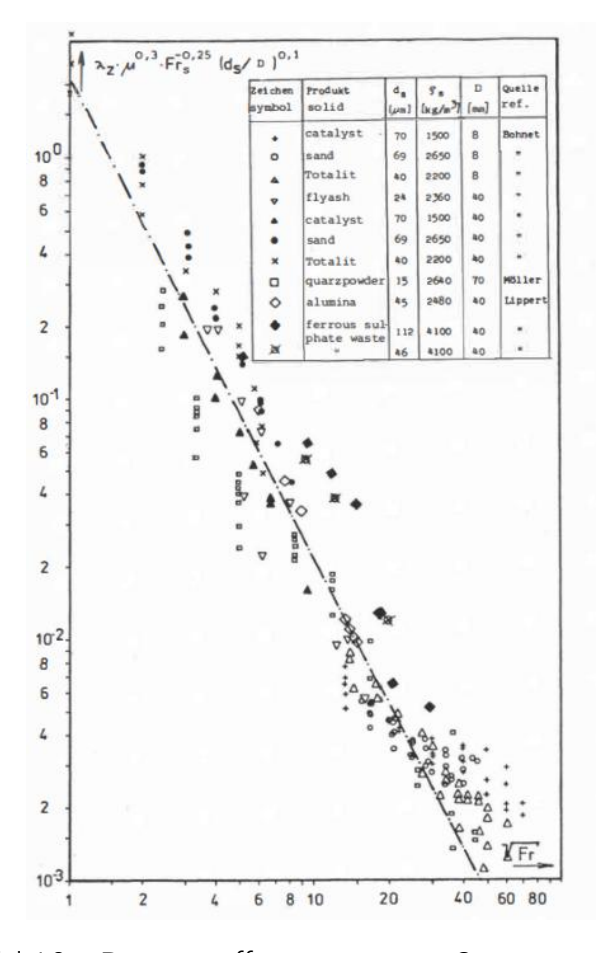


Bild 10: Drag coefficients acc. to Stegmaier for fine-grained products [10, 33]

Figure 11 shows an example of the resistance coefficients of two polystyrene granules plotted against the Froude number Fr_R . It can be seen that the coefficient of drag λ_S is not a constant and is dependent on other factors. Figure 11 shows the dependence on the load μ and the pipe diameter d_R .

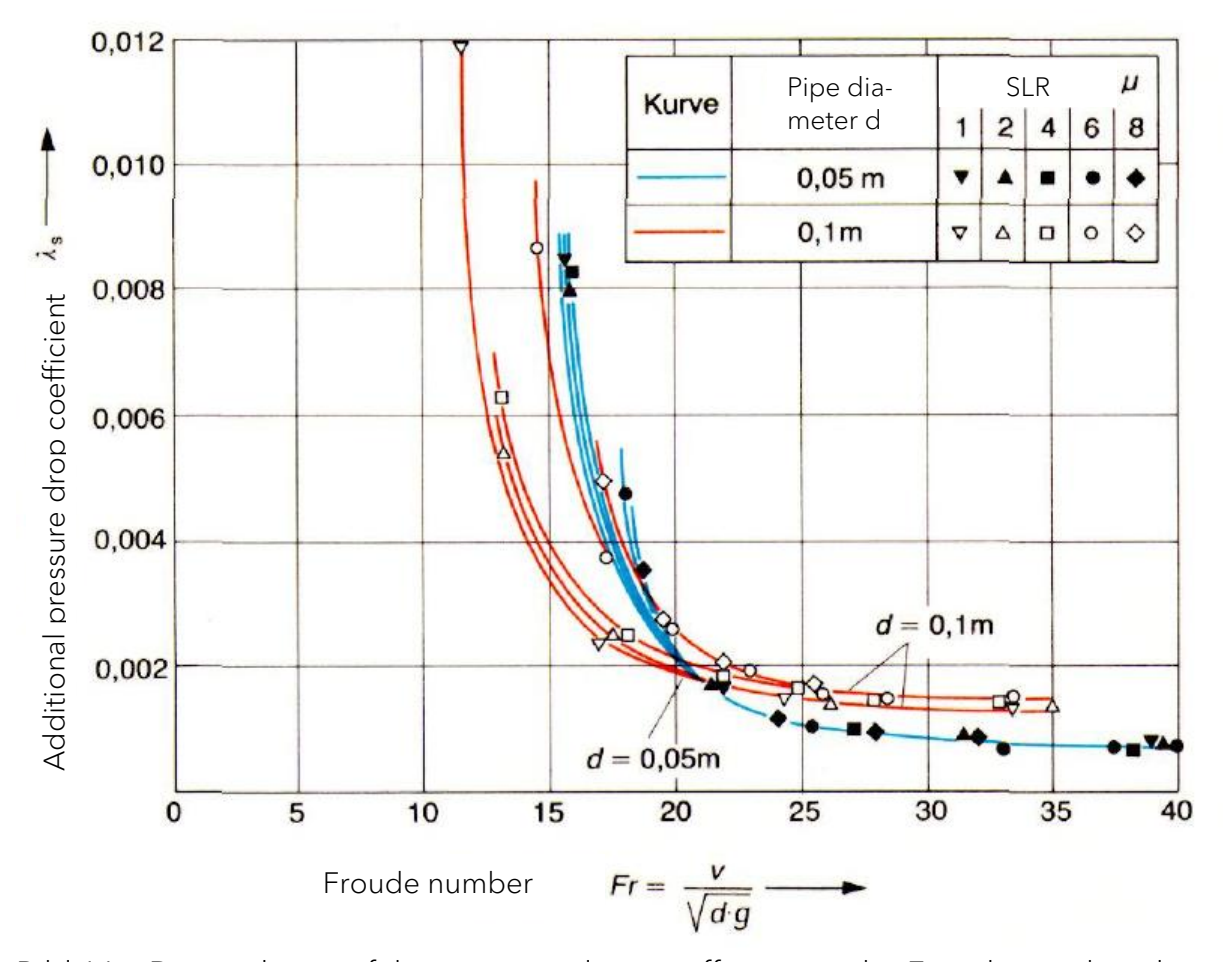


Bild 11: Dependence of the pressure drag coefficient on the Froude number during horizontal conveying of two polystyrene granulates ($d_{50} = 1.27$ mm, 2.70 mm) in pipes with diameters of 50 and 100 mm, according to [17, 32]

Siegel [2] has published resistance coefficients based on his own and third-party measurements in his book. He specifies a resistance coefficient for each bulk material listed. He specifies these values as a linear dependency of the pipe diameter. However, practice shows that the resistance coefficients:

- 1. are not constant,
- 2. are dependent on the Froude number,
- 3. are dependent on the SLR,
- 4. are dependent on the pipe diameter,
- 5. the dependence of points 2 4 can be exponential, so the exponent 1, which he chose for dependence on the pipe diameter, is primarily applicable to granulates. For fine bulk solids, the exponent deviates from 1.

This inaccuracy of the calculation must be countered with sufficient reserves.

3.3.5 Pressure loss of the vertical bulk solid transport

The pressure loss of the vertical flow dp_{ve} is made up of two components. Firstly, the pressure loss due to bulk material/bulk material contacts, bulk material and gas wall friction and secondly, the lifting pressure loss for bulk material and gas, whereby the latter can generally be neglected. Figure 12 shows the force balance on the vertical pipe element. The relevant forces are:

• Bulk solid friction: $F_{S,S}$

• Wall friction: $F_{S,R}$

• Drag force due to particle flow: $F_{S,W}$

• Pressure forces: F_P

• Buoyant force: $F_{S,A}$

• Weight force: $F_{S,G}$

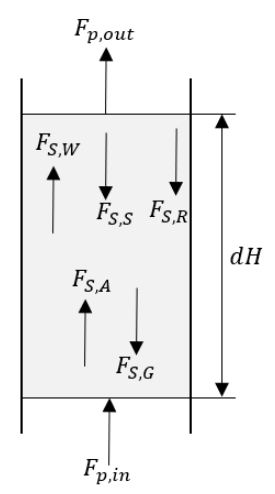


Bild 12: Force balance on a vertical pipe element on the bulk material

The sliding friction $F_{S,R}$ on the pipe wall is negligibly small. Based on measurements [34], the solid friction $F_{S,W}$ corresponds to 0.45...0.5 times the horizontal friction in the dense flow range:

$$-dp_{ve,S,W} = (0.45 \dots 0.50) \cdot \varepsilon_F \cdot \mu \cdot \lambda_{S,ve} \cdot \frac{dH_R}{d_R} \cdot \frac{\rho_F}{2} \cdot v_F^2$$
(33)

For the lifting energy, the mass of bulk material in the vertical section must be supported by the pressure difference. Using Eq. (12) and Eq. (27), the vertical pressure loss follows from the force balance:

$$-dp_{S,ve,Hub} = \varepsilon_F \cdot g \cdot \mu \cdot \rho_F \cdot \frac{dH_R}{c_{SL}} \tag{34}$$

The total vertical pressure loss $dp_{S,ve}$ can be calculated by adding Eq. (33) and Eq. (34):

$$-dp_{S,ve} = \left(\varepsilon_F \cdot \mu \cdot \rho_F \cdot dH_R\right) \cdot \left(\frac{g}{c_{SL}} + \left(0.45 \dots 0.50\right) \cdot \frac{\lambda_S}{d_R} \cdot \frac{v_F^2}{2}\right) \tag{35}$$



Further calculation approaches for the vertical pressure loss or for the drag coefficient, usually specific to bulk solids, can be found in [36 - 41].

3.3.6 Summary of all pressure loss terms

The individual terms can be determined according to Table 1:

Namibg	Formula
Total pressure loss	$-\Delta p_{ges} = \Delta p_{F,ges} + \Delta p_{ac} + \Delta p_{ve} + \Delta p_{fi} + \Delta p_{ho} + \Delta p_{be}$
Pressure loss conveying gas	$-\Delta p_{F,ges} = \sum_{i} \left(\varepsilon_{F} \cdot \lambda_{F} \cdot \frac{\rho_{F}}{2} \cdot v_{F}^{2} \cdot \frac{L_{R}}{d_{R}} \right) + \sum_{j} \left(\lambda_{E} \cdot \frac{\rho_{F}}{2} \cdot v_{F}^{2} \right) + \Delta p_{F,ac} \ (\approx 0) + \Delta p_{F,ve} (\approx 0)$
Pressure loss solid acceleration	$-\Delta p_{ac} = arepsilon_F \cdot c_{sL} \cdot \mu \cdot ho_F \cdot v_F^2$
Vertical bulk solid pressure drop	$-\Delta p_{ve} = (\varepsilon_F \cdot \mu \cdot \rho_F \cdot H_R) \cdot \left(\frac{g}{c_{SL}} + (0.45 \dots 0.50) \cdot \frac{\lambda_S}{d_R} \cdot \frac{v_F^2}{2}\right)$
Loss of solid pressure due to fittings	$-\Delta p_{fi} = \sum_{k} \lambda_{fi} \cdot \frac{\rho_F}{2} \cdot v_F^2$
Horizontal solid pressure loss	$-\Delta p_{ho} = \varepsilon_F \cdot \mu \cdot \lambda_S \cdot \frac{L_R}{d_R} \cdot \frac{\rho_F}{2} \cdot v_F^2$ (\lambda_S is to be determined on the basis of practical tests)
Pressure loss due to bends	$-\Delta p_{be} = (1 - \varepsilon_F) \cdot \mu \cdot v_F \cdot \rho_F \cdot (v_{s,out} - v_{s,in})$
Solid loading ration SLR	$\mu = \frac{\dot{m}_S}{\dot{m}_F} = \frac{\dot{V}_S \cdot \rho_S}{\dot{V}_F \cdot \rho_F} = \frac{(1 - \varepsilon_F) \cdot v_S \cdot \rho_S \cdot A_R}{\varepsilon_F \cdot v_F \cdot \rho_F \cdot A_R}$
Slip factor	$c_{SL} = \frac{v_S}{v_F} = 1 - \frac{w_{Tr}}{v_F}$ $w_{Tr} = 2,28 \cdot \frac{\eta_F}{d_S \cdot \rho_F} \cdot Ar^{0,419}$ $Ar = \frac{d_{S,50}^3 \cdot g}{\eta_F^2} \cdot \rho_F \cdot (\rho_P - \rho_F)$
Void	$1 = \varepsilon_F + \varepsilon_S$

Tabelle 1: Pressure loss terms of a pneumatic conveying system

Experimental investigations are necessary as the drag coefficient λ_S cannot be determined on the basis of mechanical bulk solids analyses, e.g. bulk density, particle density, particle size distribution. The situation is similar with the minimum initial conveying gas velocity. It must be determined in conveying tests in order to avoid pipework blockages.

4 Inhalt der VT - Toolbox

The toolbox primarily contains the design of continuous pneumatic conveying systems. The feed devices, such as pressure vessels, jet feeders or screw pumps, are not dimensioned with the toolbox. The following programmes are available for pneumatic conveying:

- Dense phase conveying of plastic granulates by Muschelknautz and Krambock
 [2]
- Dilute and strand conveying based on the drag coefficient calculation by Siegel [3]
- Dilute and strand conveying based on the drag coefficient calculation by Stegmaier for fine bulk solids ($d_{s,50} < 150 \mu m$) [4]
- Dilute and strand conveying based on the Scale-Up Model of Hilgraf [46]
- Vacuum conveying: Dilute phase transport based on the drag coefficient of Siegel [3]
- Vacuum conveying: Dilute phase transport based on the drag coefficient of of Stegmaier for fine bulk solids ($d_{s,50}$ < 150 μ m) [4]

In addition to the calculation approaches for pneumatic conveying, the VT-Toolbox contains the following modules, which are intended to make daily work easier:

- - Thermal expansion of pipeline
- - Velocities in pipelines
- Conversion of velocities and volume flows as a function of pressure and temperature
- Particle settling velocity
- - Pipe table according to DIN 10220, welded (replacement for DIN 2458)
- Fluidization point velocity
- Decision matrix for bulk solids transport
- Rotary valve design according to ISO 3922
- - Pressure loss calculation for air pipes
- Geldart-Diagramm (in progress)



5 Using the Toolbox (Pneumatic conveying)

5.1 Entering the conveying line routing

All pneumatic calculation pmodules require the same input of the conveying line pipe routing. The pipe routing data must be entered below the system data and input area. The routing is divided into the following areas:

- Horizontal length [m]
- Vertical height [m]
- 90° bends [-]

Inclined pipe runs (gradient angle $> 5^{\circ}$) are not permitted.

Negative vertical conveying lines (e.g. from surface to underground) cannot be calculated with the programme. Negative height input is not permitted. Short negative conveying lines must be entered as lifting distances. The energetic pressure recovery is only relevant from loads > 35 and several hundred metres.

The programme allows you to use up to 30 pipe sections (Fig. 14). The system does not have to be divided into 30 sections. It is therefore not necessary to fill in all 30 sections. Where no value is entered, a 0 "zero" should be entered or no value should be entered.

Either a horizontal length, a vertical height or a 90° bend should be entered for each section. This increases the accuracy of the calculation. Several entries should therefore not be made in one section. This is possible but reduces the calculation accuracy slightly.

Values other than "1" can be entered for the bends. A 45° bend can therefore be entered with the value 0.5, a 30° bend with the value 1/3.

For pneumatic conveying that are operated with positive pressure, the piping route must be entered from the back to the front. This means that the last pipe section of a conveying line must be entered in the first line.

For suction conveying calculations, the beginning of the conveying line must be entered in the first line, i.e. the other way round than for pressure conveying. The reason for this lies in the calculation process.

It is recommended to enter the horizontal and vertical lengths with a maximum of 10 m per section. This increases the accuracy of the calculation.

The clear length of the bend must be taken into account in the horizontal and vertical lengths.



For overpressure conveying systems according to Siegel, Hilgraf and Stegmeier, it is possible to calculate a staggered pipeline. In contrast to the other calculation approaches, the pipe diameter must be entered in the area of the pipe sections. The pipe diameter must therefore be specified for each calculation section. If pipe diameter jumps (staggering) are entered, the programme checks these for meaningfulness.

In the calculation approaches mentioned above, the staggering limit is also checked. As this depends on the pipe diameter, it is checked for each pipe section (see Fig. 13). The test result is represented by a red cell colour. In the Stegmaier approach, a loading limit factor is calculated in addition to the staggering limit. If the loading exceeds an upper limit value, this is also shown by a red cell colour.

Section	Horizontal length [m]	Vertical height [m]	Number of 90° bends [-]	Inner pipe diameter [m]	Control of pipe staggering [-]	Local pressure [Pa]	Pipe blockage velocity [m/s]	Loading limit factor of the plugging limit [-]	Local velocity [m/s]
End of conveying line	0	0	0	0.150		101325		0.015	24.00
Section 1			1	0.150	1.00	101325	11.29	0.015	24.00
Section 2	5			0.150	1.00	106276	11.09	0.015	22.88
Section 3		9		0.150	1.00	107628	11.04	0.015	22.60
Section 4		9		0.150	1.00	110111	10.95	0.016	22.09
Section 5			1	0.150	1.00	112651	10.86	0.016	21.59
Section 6	10			0.150	1.00	117096	10.71	0.017	20.77
Section 7	10			0.150	1.00	120075	10.61	0.017	20.25
Section 8	10			0.150	1.00	123130	10.52	0.018	19.75
Section 9	10			0.150	1.00	126263	10.42	0.018	19.26
Section 10	10			0.150	1.00	129475	10.33	0.019	18.78
Section 11	10			0.150	1.00	132769	10.24	0.019	18.32
Section 12	10			0.150	1.00	136147	10.15	0.020	17.86
Section 13	10			0.150	1.00	139610	10.06	0.020	17.42
Section 14	10			0.150	1.00	143162	9.97	0.021	16.99
Section 15	10			0.150	1.00	146805	9.89	0.021	16.57
Section 16	10			0.150	1.00	150540	9.80	0.022	16.15
Section 17			1	0.150	1.00	154369	9.71	0.022	15.75
Section 18		6		0.150	1.00	157591	9.65	0.023	15.43
Section 19			1	0.150	1.00	160024	9.59	0.023	15.20
Section 20	6			0.150	1.00	163130	9.53	0.023	14.91
Section 21				0.150	1.00	165620	9.48	0.024	14.68
Section 22				0.150	1.00	165620	9.48	0.024	14.68
Section 23				0.150	1.00	165620	9.48	0.024	14.68
Section 24				0.150	1.00	165620	9.48	0.024	14.68
Section 25				0.150	1.00	165620	9.48	0.024	14.68
Section 26				0.150	1.00	165620	9.48	0.024	14.68
Section 27				0.150	1.00	165620	9.48	0.024	14.68
Section 28				0.150	1.00	165620	9.48	0.024	14.68
Section 29				0.150	1.00	165620	9.48	0.024	14.68
Section 30				0.150		165620	9.48	0.024	14.68
Acceleration	0	0	0	0.150		165620			14.68
Air Pressure Drop	0	0	0	0.150		170113			14.30
Backpressure	0	0	0	0.150		176415			13.79
Sum	121.0000	24.0000	4.0000						

Bild 13: Sectional input of the conveying line routing

Figure 14 shows an example of a pipe routing as shown in Figure 13.

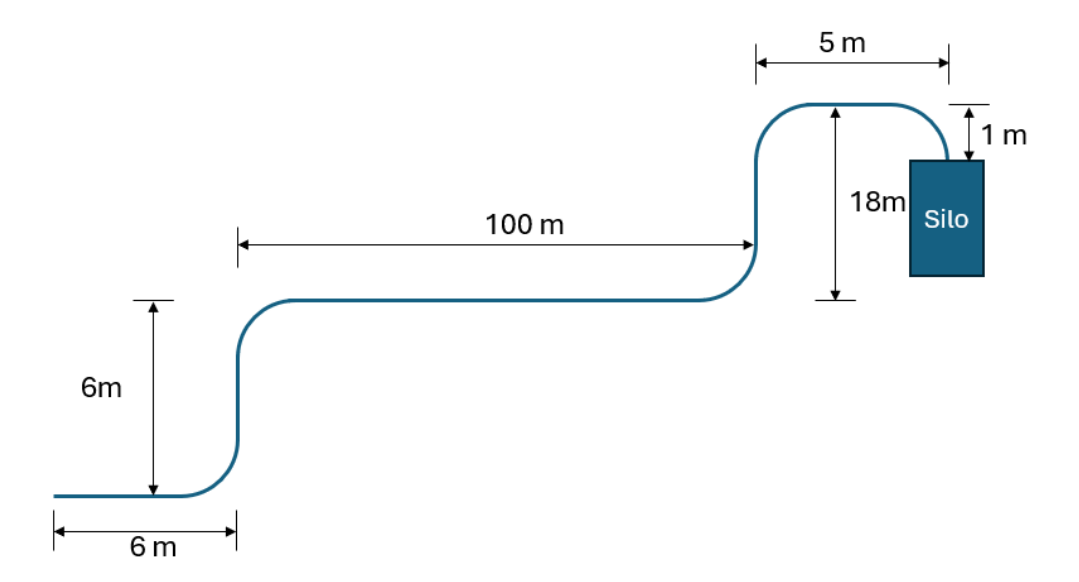


Bild 14: Example of a pipe routing

At the end of the table, the horizontal sections, the vertical sections and the number of equivalent 90° bends are added together. This is used to check the input.

5.2 Dense phase conveying of plastic granules acc. Muschelknautz and Krambock

The dimensioning of the dense flow requirement of plastic granulate is calculated according to [2]. With this conveying method, plugs are conveyed through the pipe. These plugs according to Fig. 6 mode F take up granulate lying in the pipe at the plug front and release it at the end of the plug, so that a layer of granulate of varying thickness always remains on the bottom of the pipe. Figure 15 shows such a conveyor. Source [44] shows a video on the flow forms using plastic granulate. The calculation approach is only valid for dry, non-sticky, pure plastic granulates without fines.

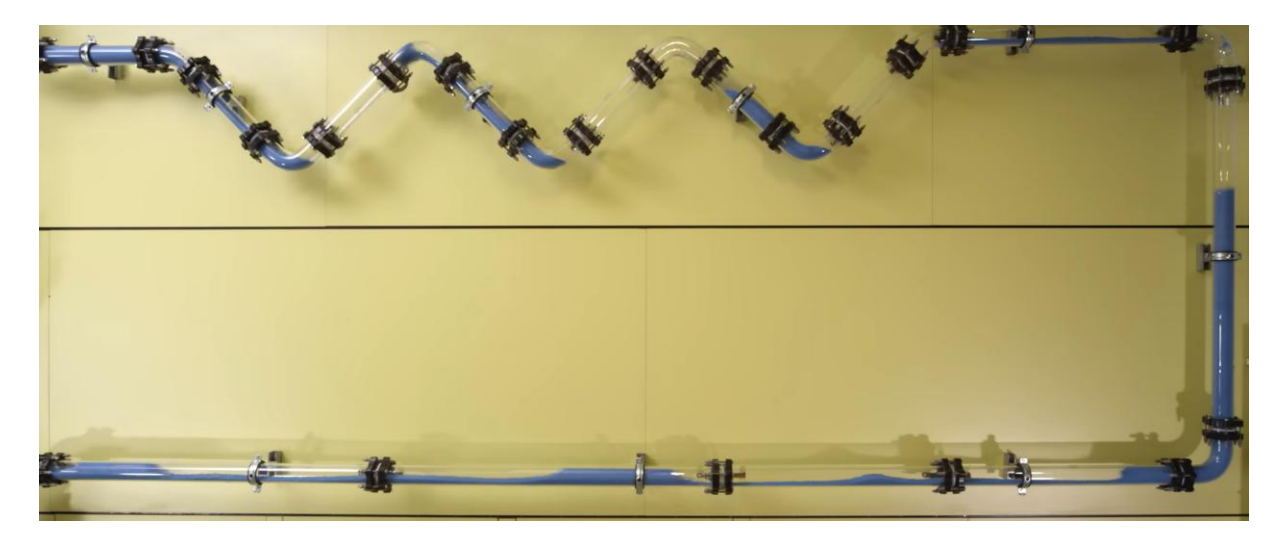


Bild 15: Dense phase conveying of plastic pellets from Coperion GmbH [44]



5.2.1 Limits of use of the programme

In addition to the limits listed below, the programme should be operated within the following limits:

Total pressure drop: \leq 6 bar(g)

Conveying line diameter: ≤ DN200 (8")

5.2.2 Entering the bulk solids data

The following additional data are required in addition to the conveying line routing in order to calculate dense phase pneumatic in accordance with [2]:

- Minimum bulk material temperature: As the calculation of the pneumatic transport is based on impulse transmission, the mass flow of the conveying gas is decisive. The mass flow rate falls when the density falls for a given volume flow rate. The density in turn falls as the conveying gas temperature rises. If the system is dimensioned with a bulk material temperature that is too high, there will be no impulse at lower bulk material temperatures. In order to reliably map all operating states, the lowest bulk solids temperature must be selected for the intended operation.
- Bulk density based on DIN ISO 697. There is no "one" bulk density. Depending
 on the process, an appropriate density must be used. This can be the bulk
 density according to DIN 51705, DIN ISO 697 or DIN 66137, for example. For
 pneumatic transport, the bulk material mass loosely filled into a container with
 a volume of 1 litre can be used as the bulk density in relation to the volume of
 1 litre. When filling, care must be taken to ensure that no bulk material bridges,
 or air pockets are formed that could distort the density.
- Conveying gas final velocity: it must be selected so that the <u>initial</u> conveying gas velocity, which is shown in the output box under "Calculation results" (Fig. 16), fulfils the condition of being > 2.5 m/s. If the condition is not met, the calculation will still be carried out and the cell will be marked "light red". If the system is built with these parameters, the pipework will become blocked. It is therefore not permitted to use this calculation result. The calculation leaves its area of validity.

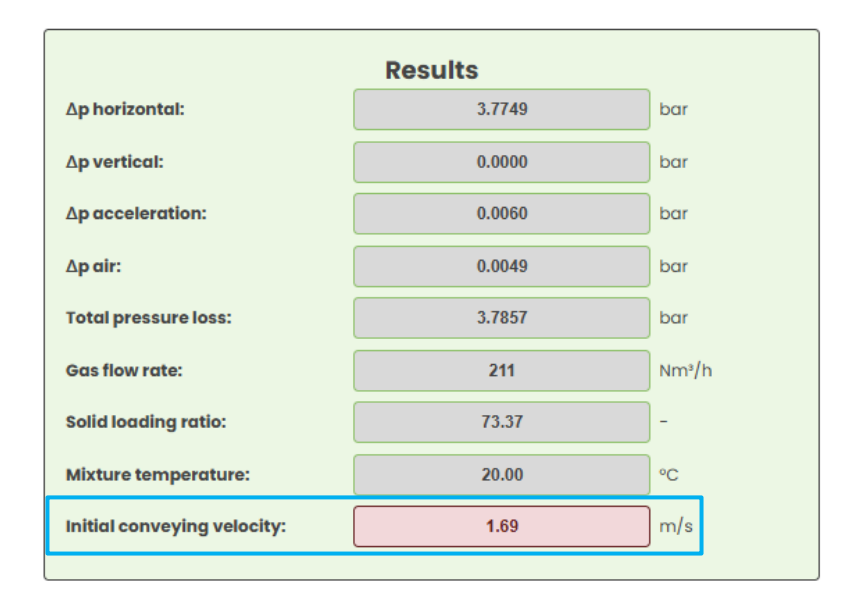


Bild 16: Check of the conveying gas initial velocity under the chapter "Results"

5.2.3 Entering the plant / system data

To perform the calculation of dense phase conveying in accordance with [2], the following additional data is required in addition to the conveying line route and the bulk solids data (Fig. 17):

- Conveying line inner diameter [mm]
- Plant altitude above sea level: The plant altitude affects the final conveying velocity. The final velocity entered by the operator in chapter 5.2.2 is corrected on the basis of the plant altitude. As the system height increases, the ambient pressure and therefore the air density decreases. As the calculation of the pneumatic transport is based on the momentum transfer, the mass flow of the conveying gas is decisive. The mass flow rate falls when the density falls for a given volume flow rate. To ensure that the required mass flow is maintained, the conveying gas velocity is automatically corrected.
- Mass flow [kg/h] of the bulk solid during the transport
- Conveying gas temperature [°C]: The mixing temperature is determined using the conveying gas temperature, the bulk material temperature, the mass flow and the specific heat capacity. This in turn is used to determine the loading. It is a decisive dimensionless parameter for determining the pressure loss. When selecting the conveying gas temperature, the operator should take into account the cooling between the pressure generator and the bulk material feed. A low conveying gas temperature is on the safe side of the calculation.
- Counter pressure [Pa]: If the pneumatic transport ends in a reactor or container with an increased internal pressure, this must be taken into account in the "Counter pressure at the end of the line" cell. The counter pressure influences the velocity and pressure loss profile of the conveying system.

System Data		
Conveying line inner diameter:	100	mm
Plant altitude:	0	m
Mass flow of bulk solid:	20000	kg/h
Conveying gas temperature:	20	°C
Ambient pressure:	1.01	bar
Counter pressure at the end of the line:	0	Pa
Pressure at the end of the line:	101325	Pa
(Final) Velocity of the gas (corrected by the plant altitude):	24.00	m/s

Bild 17: Plant data and system data of the conveying system

5.2.4 Calculation results

Figure 18 shows the calculation results. The following data are shown:

- 1. Sum of horizontal pressure drop [bar(g)]: Δp horizontal
- 2. Sum of vertical pressure drop [bar(g)]: Δp vertical
- 3. Pressure drop of bulk solid acceleration [bar(q)]: Δp acceleration
- 4. Pressure drop o fair flow [bar(g)]: Δp air
- 5. Total pressure loss [bar(g)]: it is the sum of the pressure losses of items 1,2,3,4. It is the back pressure, without additional pressure losses, such as pulsations, air pipe pressure losses, pressure losses for e.g. coolers, dryers, separators etc.
- 6. Conveying gas volume flow [Nm³/h (0 °C, 1.013bar(abs.))]. This is the amount of conveying gas that is required for pneumatic transport in the conveying pipe after the feeding unit. Additional air volumes, such as the leakage air of a rotary valve, are not taken into account in this air volume. They must be considered separately by the operator depending on the feeding device. It should also be noted that the conveying gas volume is specified at 0 °C and 1.013 bar(abs.), i.e. standard conditions in accordance with DIN1343. Pressure generator suppliers often specify the air volume at 20 °C. This is a difference of 7.3 % air volume. It is therefore important to ensure that the reference conditions are specified.
- 7. Solid loading ratio: This is the ratio of bulk solids mass flow to conveying gas mass flow in the unit [-].



- 8. Mixing temperature: This is the mixing temperature at the beginning of the conveying line between the conveying gas and the bulk material. Radiated heat via the pipe is not taken into account.
- 9. Initial conveying gas velocity: It must be > 2.5 m/s for dense phase conveying of plastic pellets. It results from the final conveying gas velocity, the mixing temperature and the pressure ratio of the final pressure (pressure at the end of the line) to the initial pressure (total pressure loss).

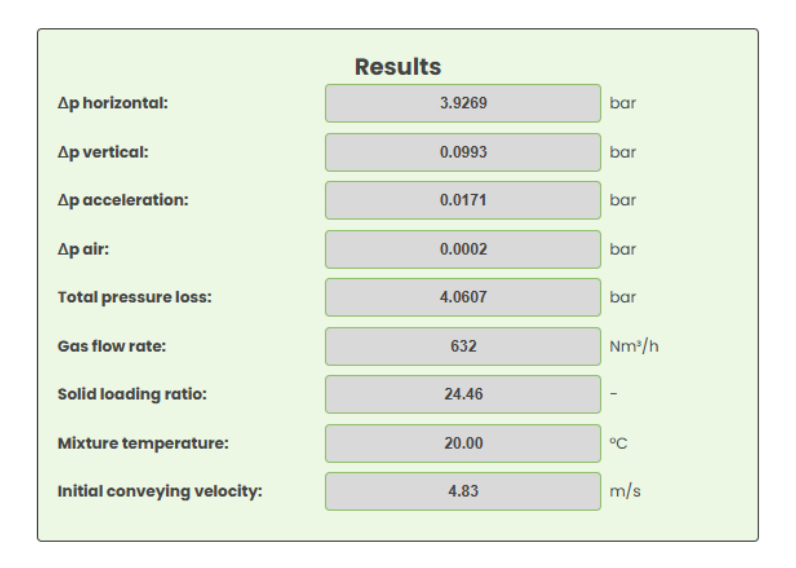


Bild 18: Calculation results

5.3 Overpressure conveying based on the drag coefficient by Siegel [3]

This chapter only explains the input and output values that differ from those in chapter 5.2.

5.3.1 Einsatzgrenzen des Programmes

In addition to the limits listed below, the programme should be operated within the following limits:

Total pressure drop: $\leq 2 \text{ bar(g)}$

Conveying line diameter: ≤ DN200 (8")

5.3.2 Input of the bulk solid data

The calculation is based on 57 bulk materials. Table 2 shows the bulk solids with the, in the program stored, bulk solids data. Except for the initial conveying gas velocity, they cannot be changed in the programme, as the resistance coefficient is permanently linked to the values.

	Average	Particle	Bulk den-		-
	particle dia-	density	sity	Initial conveying	Drag coeffi-
Bulk solid	meter [mm]	[kg/m³]	[kg/m³]	gas velocity [m/s]	cient λ_{s}
Field beans	8,1	1390	830	23-27	0,04
Activated carbon	0,003	1860	340	20-23	0,06
Bentonite	0,04	2680	720	25-27	0,1
Bitter lupins	6,1	1340	830	23-27	0,04
Barley	4	1420	690	20-25	0,04
Glas beads	1,14	2990	1780	22-27	0,06
Mica, calcined	2	2520	100	18-22	0,03
Mica, raw	0,93	2550	830	25-30	0,09
Green malt	4,5	1320	400	23-27	0,06
Oats	3,4	1340	510	22-25	0,04
Wooden slats	100x50x4	720	500	23-27	0,08
Wooden shavings	50 x 20 x 1	470	150-400	22-25	0,04
Wood wool	200 x 3 x 3	470	20	20-25	0,04
Bird's-foot trefoil	1,1	1420	830	22-25	0,04
Potato flakes	10 x 10 x1	1200	300	20-23	0,04
Concentrated feed	0,86	1370	540	22-25	0,06
Corn, moist	8,7	1250	680	22-27	0,06
Corn, dry	7,7	1300	680	22-25	0,04
Cornmeal	0,75	1440	650	23-25	0,06
Cornflour	0,19	1400	460	23-25	0,1
Makrolon granules	3,2	1230	670	22-25	0,04

Malz	3,7	1370	540	20-22	0,04
Malt grist	0,7	1480	400	22-25	0,06
Methylcellulose	0,35	1230	370	22-25	0,06
Sodium bicarbonate	0,063	2700	1070	22-25	0,1
Cardboard tubes	100x20	970	50	18-20	0,04
Phenolic resin	0,65	1380	520	20-25	0,06
Polyethylene granules	3,5	1070	500	20-25	0,04
Polyethylene powder	0,25	1070	450	20-25	0,1
Polyester chips	6 x 4 x 2	1400	700	23-27	0,06
Polypropylene gra-					
nules	3,5	1000	500	20-25	0,04
Polypropylene pow-					
der	0,22	1000	570	20-25	0,1
Polystyrole granules	3,5	1070	600	20-25	0,04
PVC powder	0,2	1320	570	20-25	0,1
Rice	2,7	1620	800	20-25	0,06
Rice husks	2,5	1280	105	18-20	0,04
Rye	3	1180	620	22-25	0,04
Sawdust	0,7	470	190	20-25	0,04
Soap noodles	20 x 5	1100	600	23-27	0,08
Soya beans	6,3	1270	690	22-25	0,04
Summer rapeseed	1,9	1140	680	20-25	0,04
Steel balls	1,08	7850	4420	25-35	0,12
Rock salt	1,6	2190	1200	22-27	0,08
Styrofoam balls	3,5	84	29	10-20	0,04
Dried distillers' grains	0,96	680	260	20-22	0,04
White mustard	2,1	1190	700	20-25	0,04
Wheat	3,9	1380	730	22-27	0,04
Wheat bran	1	1470	300	20-25	0,06
Wheat flour	0,09	1470	540	18-23	0,08
Wheat middlings	0,15	1470	370	20-25	0,06
Winter vetche	3,4	1390	820	22-25	0,04
Cellulose powder	0,04	1380	230	20-25	0,04
Cement	0,05	3100	1420	20-25	0,15
Cement raw meal	0,05	3100	960	20-25	0,13
Chicory	25	1320	300	23-27	0,06
Zinc oxide	0,1	4850	2000	25-30	0,15
Sugar	0,52	1610	860	20-25	0,08

Tabelle 2: Bulk solids data acc. [3]

Figure 19 shows that the bulk material to be conveyed can be selected via a drop-down field. Once the bulk material has been selected, the fields:

- Drag coefficent
- Bulk density
- Particle density

automatically filled.



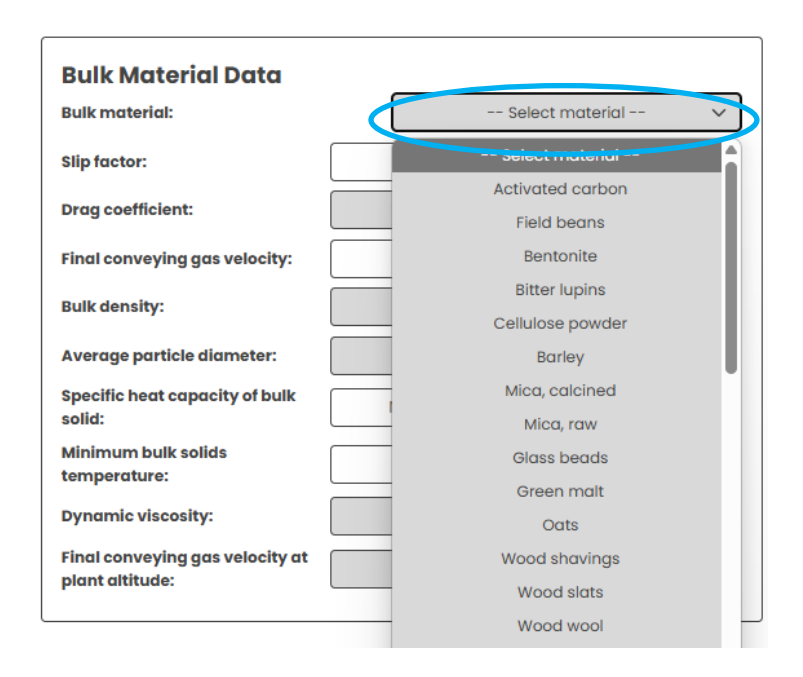


Bild 19: Selection oft he bulk material

- Slip factor: It is the ratio of bulk material velocity to conveying gas pipe velocity. If the slip is not known, it should be set to 0.7.
- Final conveying gas velocity: For fine bulk solids ($d_{5,50} \le 150 \, \mu m$), the final velocity should be selected so that the pipe blockage velocity (blue frame) in the table of pipe sections entered (Fig. 20) is always at least 3 m/s above the local velocity (green frame). Regardless of the Siegel data, we recommend the following conveying gas velocities for **fine bulk solids** depending on the conveying line back pressures up to 1.0 bar(g) (the velocity must be increased with increasing conveying line back pressure or increasing bulk density > 1000 kg/m³):
 - $o \leq DN80 (3''): > 18 \text{ m/s}$
 - o DN80 (3") ... DN100 (4"): > 20 m/s
 - o DN100 (4") ... DN125 (5"): > 22 m/s
 - o DN125 (5") ... DN150 (6"): > 23 m/s
 - o DN150 (6") ... DN200 (8"): > 24 m/s

Section	Horizontal length [m]	Vertical height [m]	Number of 90° bends [-]	Inner pipe diameter [m]	Control of pipe staggering [-]	Local pressure [Pa]	Local velocity [m/s]	Local density [kg/m²]	Pipe blockage velocity [m/s]
End of conveying line	0	0	0	0.100		101325	24.00	1.205	6.96
Section 1			1	0.100	1.00	101325	24.00	1.205	6.96
Section 2	6			0.100	1.00	107266	22.67	1.276	6.85
Section 3			1	0.100	1.00	110153	22.08	1.310	6.80
Section 4		9		0.100	1.00	115618	21.03	1.375	6.71
Section 5		9		0.100	1.00	121868	19.95	1.449	6.62
Section 6			1	0.100	1.00	128244	18.96	1.525	6.52
Section 7	10			0.100	1.00	132939	18.29	1.581	6.46
Section 8	10			0.100	1.00	136820	17.77	1.627	6.41
Section 9	10			0.100	1.00	140592	17.30	1.672	6.37
Section 10	10			0.100	1.00	144262	16.86	1.716	6.32
Section 11	10			0.100	1.00	147839	16.45	1.758	6.28
Section 12	10			0.100	1.00	151330	16.07	1.800	6.24
Section 13	10			0.100	1.00	154739	15.72	1.840	6.21
Section 14	10			0.100	1.00	158074	15.38	1.880	6.17
Section 15	10			0.100	1.00	161339	15.07	1.919	6.14
Section 16	10			0.100	1.00	164537	14.78	1.957	6.11
Section 17			1	0.100	1.00	167673	14.50	1.994	6.08
Section 18		6		0.100	1.00	171264	14.20	2.037	6.05
Section 19			1	0.100	1.00	176356	13.79	2.097	6.01
Section 20	6			0.100	1.00	179770	13.53	2.138	5.98
Section 21				0.100	1.00	181492	13.40	2.159	5.96

Bild 20: Check of the pipe blockage velocity

• Final conveying gas velocity: For granulates (d_{s,50} ≥ 150 μm), the final velocity should be selected so that the recommended initial conveying gas velocity in the "System data" field (green marking in Fig. 22) is reached. The actual initial conveying gas velocity of the calculation is shown in the green area of the Results (blue marking in Fig. 21). The lower velocity refers to pipes ≤ DN80, the upper specification to pipes of size DN200. The initial conveying gas velocity is shown under Calculation results (Fig. 21). The check is not carried out automatically. It must be carried out by the operator. The final conveying gas velocity must be adjusted until the condition described above is fulfilled.

Results								
Δp horizontal:	0.3934	bar						
∆p vertical:	0.1772	bar						
Δp bend:	0.2311	bar						
Δp acceleration:	0.0663	bar						
Δp air:	0.0863	bar						
Total pressure loss:	0.9543	bar						
Conveying gas volume flow:	632	Nm³/h						
Solid loading ratio:	24.46	-						
Mixture temperature:	20.00	°C						
Initial conveying gas velocity:	12.36	m/s						

Bild 21: Results

• Specific heat capacity: This is used to determine the mixing temperature. If the specific heat capacity is not known, a value of 750 J/kg/K can be used. The following list shows the specific heat capacities of various bulk materials:

Fly ash: 840 J/(kg·K) Cement: 750 J/(kg·K) Wood: 2100 J/(kg·K) Chipboard: 2100 J/(kg·K) Concrete: 1000 J/(kg·K) Polyurethan: 1500 J/(kg·K) Polystyrene: 1500 J/(kg·K) Sheep's wool: 1300 J/(kg·K) Mineral wool: $800 J/(kg\cdot K)$ Sulphur: 720 J/(kg·K) Aluminium: 921 J/(kg·K)

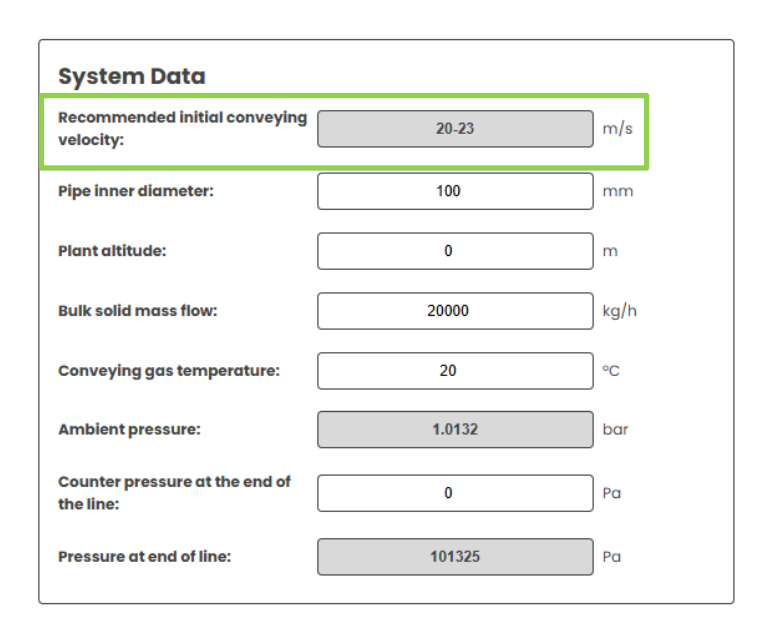


Bild 22: System data

5.4 Vacuum conveying based on the drag coefficients by Siegel [3]

This section only explains the input and output values that differ from those in sections 5.2 and 5.3.

5.4.1 Limits of the program module

In addition to the limits listed below, the programme should be operated within the following limits:

Total pressure drop: ≤ 0.75 bar(g)

Conveying line diameter: ≤ DN200 (8")

The programme allows calculation outside the limits listed above. In this case, the calculations must be compared with process engineering experience.

5.4.2 Bulk solid input data

The only difference to the input data from chapter 5.3 is the input for the conveying velocity. The velocity at the start of the conveying line is the lowest velocity along the conveying line for both pressure and vacuum conveying. The pressure drops along the line and the velocity therefore increases. Small loads should be used for vacuum conveying. The initial velocity recommended in the programme (Fig. 22) must be selected. It should be selected irrespective of the fineness of the bulk material. The loading is determined using the conveying gas velocity, the pipe diameter and the bulk material mass flow. If the load exceeds a limit load that is determined in the "System data" area (Fig. 23), a comment field is displayed below the input data. To correct the process data:

- to increase the initial conveying velocity, or
- the inside diameter of the pipe is raised, or
- to reduce the mass flow.

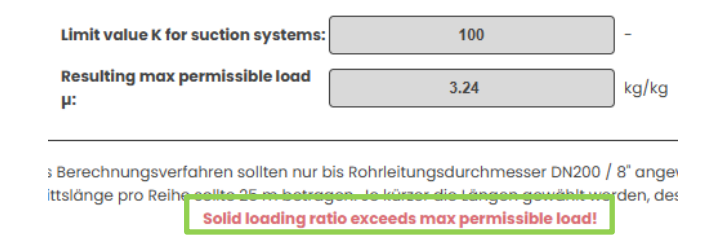


Bild 23: Calculation field for the max. permissible load for vacuum conveying under "System data"



Bild 24: Calculation results with exceeded bulk solid load

5.5 Overpressure conveying based on the calculation of Stegmaier's drag coefficient for fine bulk solids (ds,50 \leq 150 μ m)

This chapter only explains the input and output values that differ from those in chapters 5.2 - 5.4.

5.5.1 Limits of the program module

In addition to the limits listed below, the programme should be operated within the following limits:

Total pressure drop: ≤ 1.0 bar(g)

Conveying line diameter: ≤ DN200 (8")

The programme allows calculation outside the limits listed above. In this case, the calculations must be compared with process engineering experience.

5.5.2 Input of the bulk solid data

• Average particle diameter: In this calculation programme, the drag coefficient is not taken as a constant from a table, it is determined using equation (32) according to [10]. It is calculated separately for each calculation section. This requires the input of the mean particle diameter d_{S,50,3}, the pipe diameter and the bulk and particle density.

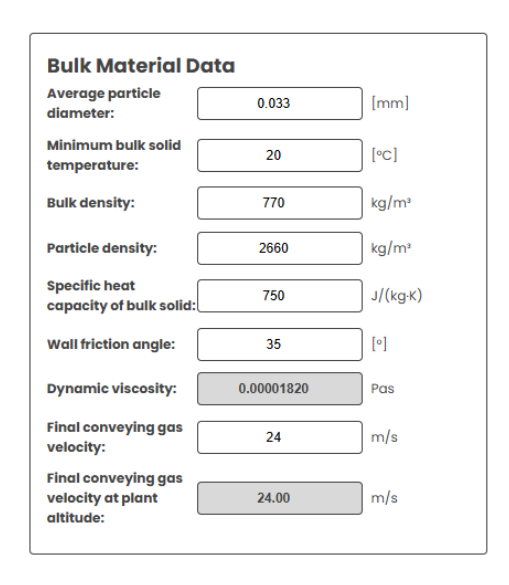


Bild 25: Input data of the bulk solid

When conveying according to Siegel, a slip factot had to be selected. In this
calculation module, the slip is calculated based on the wall friction. The wall
friction angle is between 15 - 35° depending on the wall material/bulk material
pairing. The finer a bulk material is, the greater the wall friction angle generally
becomes. However, other factors such as grain shape, density, moisture, grain

size distribution etc. also influence the wall friction angle. The wall friction angle can be determined using the Jenike shear tester [45]. If the operator does not have a value for the wall friction angle, it should be set to 25° - 30° for stainless steel pipes and 30° - 35° for mild steel pipes.

• Final conveying gas velocity: This must be specified. After entering all the data, the pipe blockage velocity must be checked in the section "Pipe blockage velocity according to Muschelknautz/Krambock" (Fig. 26). If the final conveying gas velocity has been set too low, the initial conveying gas velocity is so low that the system will block. If all cells of the "Pipe blockage velocity" and "Loading limit factor of the plugging limit" are greyed out, then the final conveying gas velocity has been selected sufficiently high. We recommend that you also comply with the final conveying gas velocity listed in chapter 5.3.2.

Section	Horizontal length [m]	Vertical height [m]	Number of 90° bends [-]	Inner pipe diameter [m]	Control of pipe staggering [-]	Local pressure [Pa]	Pipe blockage velocity [m/s]	Loading limit factor of the plugging limit [-]	Local velocity [m/s]
End of conveying line	0	0	0	0.150		101325	232.97	0.019	24.00
Section 1			1	0.150	1.00	101325	10.27	0.019	24.00
Section 2	6			0.150	1.00	106160	10.10	0.020	22.91
Section 3			1	0.150	1.00	108273	10.04	0.020	22.46
Section 4		9		0.150	1.00	112786	9.89	0.021	21.56
Section 5		9		0.150	1.00	115816	9.80	0.022	21.00
Section 6			1	0.150	1.00	118929	9.71	0.022	20.45
Section 7	10			0.150	1.00	123019	9.60	0.023	19.77
Section 8	10			0.150	1.00	127100	9.49	0.024	19.13
Section 9	10			0.150	1.00	131316	9.39	0.025	18.52
Section 10	10			0.150	1.00	135672	9.28	0.025	17.92
Section 11	10			0.150	1.00	140173	9.18	0.026	17.35
Section 12			1	0.150	1.00	144822	9.08	0.027	16.79
Section 13		6		0.150	1.00	148146	9.01	0.028	16.42
Section 14			1	0.150	1.00	150816	8.96	0.028	16.13
Section 15				0.150	1.00	154000	8.90	0.029	15.79
Section 16	6			0.150	1.00	154000	8.90	0.029	15.79
Section 17				0.150	1.00	15/065	8.84	0.029	15.48

Bild 26: Table of the pipe routing with data of the pipe blockage velocity

5.5.3 Intermediate calculations

In the "Intermediate calculations" section, calculations are performed to determine parameters for the drag coefficient and slip factor.

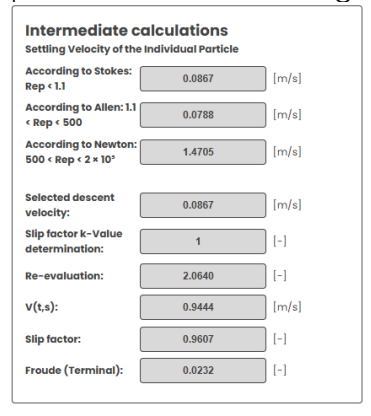


Bild 27: Intermediate calculations

5.6 Vacuum conveying based on the calculation of the Stegmaier drag coefficient for fine bulk solids ($d_{s,50} \le 150 \mu m$)

5.6.1 Limits of the program module

In addition to the limits listed below, the programme should be operated within the following limits:

Total pressure drop: ≤ 0.5 bar(g)

Conveying line diameter: ≤ DN200 (8")

The programme allows calculation outside the limits listed above. In this case, the calculations must be compared with process engineering experience.

5.7 Evaluation of the results

The calculation programmes give three primary results:

- Pipe diameter
- Total pressure loss
- Conveying gas velocity / volume flow

These results relate exclusively to the conveying line. Additional pressure losses due to e.g:

- Air ducts
- Non-return valves
- Spark arresters
- Air cooler
- Dryers
- Condensate separator
- Cyclone separator
- Pressure vessel pipework
- Nozzles of screw pumps

are not included in the calculation. They must be determined separately.

Additional air volumes such as leakage air volumes from rotary valves or drying air volumes from adsorption dryers are also not included in the calculation. They must be determined separately.

We recommend designing the pressure generator as follows:

Druck:

- 1. total pressure loss from the calculation of the respective calculation programme
- 2. addition of 15 % pressure fluctuations



- 3. addition of 20 % design inaccuracy
- 4. addition of additional pressure losses listed above
- → this leads to the nominal pressure of the pressure generator

Volume flow:

- 1. conveying gas volume flow from the calculation of the respective calculation programme
- 2. addition of additional volume flows, such as air leakage volume
- → this leads to the standard volume flow of the pressure generator

5.8 Remarks on the design of blowers and compressors

When designing the pressure generator, they utilise the installed drive power of the selected machine. Figure 30 shows the result of a blower sizing with the AERZEN web configurator (www.aerzen.com) [All well-known pressure generator suppliers provide such sizing tools]. The result shows a GM25S. The blower size (blower stage) specifies the design limit of the volume flow. However, each blower/compressor stage has a minimum and maximum air volume. Example: The data entered by the operator has resulted in a fan as shown in Fig. 30 (left). The installed motor has an output of 37 kW. However, the clutch output is "only" 30.6 kW. This pressure generator is therefore supplied in such a way that it can deliver an air volume of 1051 Nm³/h at a pressure difference of max.750 mbar. However, if there is a lack of air volume or pressure difference in the pneumatic conveying system, the blower will not be able to supply this for the time being. The blower would have to be modified (replacement of the belt drive, gearbox and/or safety valve). Design the pressure generator so that the motor is fully utilised. You can purchase the blower with more air volume or more pressure reserve at the same cost with the same motor. To do this, you must adapt the design accordingly. Fig. 30 (right) shows the same blower with the same motor with 120 mbar more pressure reserve. Please note that this does not affect the pneumatic delivery. A blower only generates the pressure and draws the motor current that it receives from the pneumatic conveying system. The additional pressure installed therefore does not affect the energy consumption of the system but increases system availability.

The selected final pressure of the pressure generator must be in line with the design limits of the overall system. If a pipework blockage occurs in the conveyor system, the maximum pressure in the system is reached. In the example above, this would be 870 mbar.

Medium	Air			Medium	Air		
Volume flow ¹	Q ₁	m³/min	19.2	Volume flow ¹	Q1	m³/min	18.9
Volume flow ¹	Q ₁	m³/h	1150	Volume flow ¹	Q ₁	m³/h	1136
Volume handled at normal condition reference to T1=273K, p1=1,013 bar, rF=0%	Qn	Nm³/h	1051	Volume handled at normal condition reference to T1=273K, p1=1,013 bar, rF=0%	Qn	Nm³/h	1038
Mass flow	m	kg/h	1375	Mass flow	ṁ	kg/h	1358
Density at inlet conditions	ρ	kg/m³	1.195	Density at inlet conditions	ρ	kg/m³	1.195
Relative humidity	rH	%	80	Relative humidity	rH	%	80
Intake pressure (abs.)	D 1	bar	1.013	Intake pressure (abs.)	p 1	bar	1.013
Outlet pressure (abs.)	D2	bar	1.763	Outlet pressure (abs.)	p ₂	bar	1.883
Pressure difference	Δp	mbar	750	Pressure difference	Δp	mbar	870
Intake temperature	t ₁	°C	20	Intake temperature	t ₁	°C	20
Discharge temperature	t ₂	°C	92	Discharge temperature	t ₂	°C	105
Male rotor speed	NHR	_	3960	Male rotor speed	NHR	rpm	3960
•	Pk	rpm kW	30.6	Power consumption at coupling	Pk	kW	35.1
Power consumption at coupling				Motor speed	NMot	rpm	2970
Motor speed	NMot	rpm	2970	Motor rating	Рмоt	kW	37
Motor rating	PMot	kW	37	_			

Bild 28: Blower data of a GM25S, the calculation was carried out online using Aerzen Webconfigurator

6 Operating the VT - Toolbox (Additional Modules)

The VT-Toolbox contains additional modules that can be used to perform calculations relating to pneumatic conveying or general process engineering calculations. These are:

- Calculation of the thermal expansion of pipework
- Calculation of velocities in pipework
- Conversion of velocities and volume flows as a function of pressure and temperature
- Calculation of the particle settling velocity
- Calculation of the loosening / fluidization point velocity
- Rotary valve design according to ISO 3922
- Pressure loss calculation of air ducts
- Geldart diagram

6.1 Calculation of the thermal expansion of pipework

This module is relevant, for example, when the expansion due to thermal conduction must be determined in relation to fixed and loose bearing points. Pipe bends that are lined with cast basalt, for example, are very sensitive to stress. If stresses occur on the bend due to thermal expansion, pipe expansion joints must be installed to absorb the thermal expansion. The amount of expansion to be absorbed must therefore be calculated. The thermal expansion ΔL of pipework is determined according to equation 36:

$$\Delta L = \alpha \cdot L \cdot \Delta T \tag{36}$$

With:

- Thermal expansion ΔL [m]
- α = Coefficient of linear/thermal expansion [1/K]
- L = Total pipework length considered [m]
- ΔT = Temperature difference between the pipework and the environment [K]

The module specifies coefficients of thermal expansion for different steels at different temperatures.

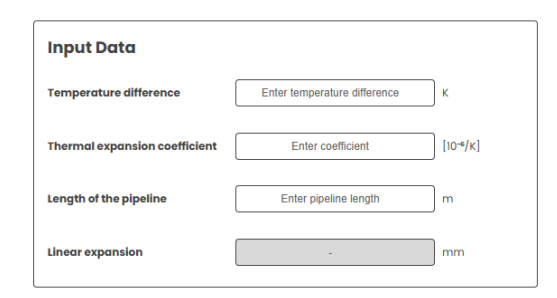


Bild 29: Module: Thermal expansion of pipes

6.2 Velocities in pipes

This module (Fig. 30) calculates the velocities in pipes. In the upper section, the velocity is determined for a specified internal pipe diameter. Below the calculation, the velocities for the standard pipe sizes from DN15 to DN600 are calculated automatically. It should be noted that the operating volume flow is the volume flow in the pipe that is related to the pressure and temperature in the pipe.

Input Data		
Operating volume flow	Enter volume flow	m³/s
Pipe diameter (clear width)	Enter pipe diameter	mm
Velocity	-	m/s

Bild 30: Module: Velocities in Pipes

6.3 Conversion of velocites and volume flows depending on the pressure and temperature

As mentioned in chapter 6.2, the operating conditions must be taken into account when determining volume flows, velocities or gas densities.

6.3.1 Standard- vs. Operational Conditions

The Boyle-Mariotte law can be used to convert operating conditions (density $\rho_{1,2}$, temperature $T_{1,2}$ and pressure $p_{1,2}$) into each other. The input level (1) can be converted to the output level (2) according to Eq. 37.

$$\frac{\rho_1 \cdot T_1}{p_1} = \frac{\rho_2 \cdot T_2}{p_2} \tag{37}$$

As a rule, the temperature T inside the pipe is assumed to be constant, so equation (38) is simplified to:

$$\frac{\rho_1}{p_1} = \frac{\rho_2}{p_2} \tag{38}$$

If volume flows rather than densities are to be converted, the volume flow can be introduced:

$$\frac{\dot{\mathbf{v}}_1 \cdot \mathbf{p}_1}{T_1} = \frac{\dot{\mathbf{v}}_2 \cdot \mathbf{p}_2}{T_2} \tag{39}$$

The term standard is often used incorrectly in this context. Standard conditions according to DIN 1343 for air, for example, are:

- $0 \, ^{\circ}\text{C} = 273.15 \, \text{K}$
- 1.01325 bar(abs.)
- 0 % relative humidity
- 1.293 kg/m³





Bild 31: Module: Boyle-Mariotte

6.3.2 Gas equation

The ideal gas equation can be used to determine pressure, density and temperature. The following additional gas data is required for this:

- General gas constant \Re [J/(mol·K)]
- Molar mass M [g/mol]
- Critical pressure pkrit: bar(abs)krit
- Critical temperature T_{krit}: [°C_{krit}]

These data are stored in the add-on module for: Argon, helium, carbon dioxide, air, methane, oxygen and nitrogen. If the corresponding gas is selected and one of the three gas data (density, pressure, temperature) is specified, the outstanding parameter is output.

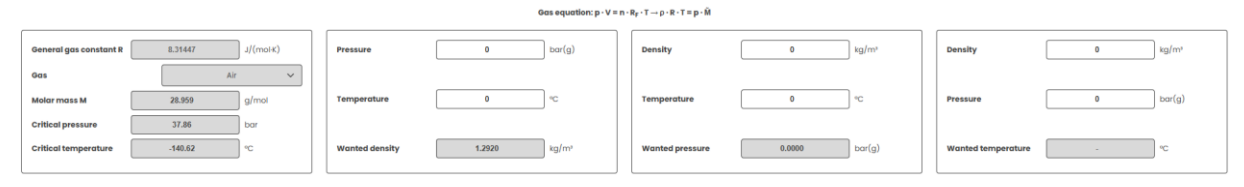


Bild 32: Modul: Gas equation

6.3.3 Plant altitude

Je höher die Anlagen über Normalnull gebaut werden soll, desto geringer ist die Luftdichte. Ein Druckerzeuger saugt eine feste Luftmenge [m³/s] an, keine Masse. Wird z.B. ein Gebläse anstatt auf 0 m auf 500 m aufgestellt, ändert sich am Gebläse die Ansaugluftmenge nicht. Die Ansaugluftmasse ändert sich in Abhängigkeit der reduzierten Dichte. Bild 33 zeigt den Berechnungsabschnitt.

The higher the plant is built above sea level, the lower the air density. A pressure generator sucks in a fixed volume of air [m³/s], not a mass. If, for example, a blower is installed at 500 m instead of 0 m, the intake air volume at the blower does not change. The intake air mass changes depending on the reduced density. Figure 33 shows the calculation section.



Bild 33: Module: Plant altitude

Table 3 shows the air pressure and air density as a function of altitude. In the add-on module, the air density and air pressure can be precisely determined by entering the altitude in relation to 15 °C. These values can be converted to other temperatures using chapter 6.3.2.

Höhe	Druck	Dichte	Höhe	Druck	Dichte	Höhe	Druck	Dichte
[m]	[bar(abs)]	[kg/m³]	[m]	[bar(abs)]	[kg/m³]	[m]	[bar(abs)]	[kg/m³]
-400	1,062	1,284	750	0,927	1,120	1900	0,809	0,978
-350	1,056	1,277	800	0,921	1,114	1950	0,804	0,972
-300	1,050	1,269	850	0,916	1,107	2000	0,799	0,966
-250	1,043	1,262	900	0,910	1,101	2050	0,794	0,960
-200	1,037	1,254	950	0,905	1,094	2100	0,790	0,955
-150	1,031	1,247	1000	0,900	1,088	2150	0,785	0,949
-100	1,025	1,239	1050	0,894	1,081	2200	0,780	0,943
-50	1,019	1,232	1100	0,889	1,075	2250	0,776	0,938
0	1,013	1,225	1150	0,884	1,069	2300	0,771	0,932
50	1,007	1,217	1200	0,879	1,062	2350	0,767	0,927
100	1,001	1,210	1250	0,873	1,056	2400	0,762	0,921
150	0,995	1,203	1300	0,868	1,050	2450	0,758	0,916
200	0,989	1,196	1350	0,863	1,044	2500	0,753	0,910
250	0,983	1,189	1400	0,858	1,037	2550	0,749	0,905
300	0,978	1,182	1450	0,853	1,031	2600	0,744	0,900
350	0,972	1,175	1500	0,848	1,025	2650	0,740	0,894
400	0,966	1,168	1550	0,843	1,019	2700	0,735	0,889
450	0,960	1,161	1600	0,838	1,013	2750	0,731	0,884
500	0,955	1,154	1650	0,833	1,007	2800	0,727	0,879
550	0,949	1,147	1700	0,828	1,001	2850	0,722	0,873
600	0,943	1,141	1750	0,823	0,995	2900	0,718	0,868
650	0,938	1,134	1800	0,818	0,989	2950	0,714	0,863
700	0,932	1,127	1850	0,813	0,983	3000	0,710	0,858

Tabelle 3: Air pressure and air density depending on the altitude

6.4 Single particle settling velocity

The terminal velocity of a single particle w_{Te} in a gas at rest is the result of the forces acting on it from drag force F_W , weight force F_G and buoyancy force F_A .

The following applies to the laminar range (Re < 1.1), the Stokes range:

$$w_{Te} = \frac{1}{18} \cdot g \cdot d_S^2 \cdot \frac{\rho_P - \rho_F}{\eta_F} \tag{40}$$

with: ρ_P = Particle density [kg/m³]

 ρ_F = Fluid density [kg/m³]

 η_F = Dynamic viscosity of the fluid [Pas]

For the transition range (1.1 $< Re_P < 500$), the Allen range, the following applies:

$$w_{Te} = \frac{18 \cdot \eta_F}{d_{S,50} \cdot \rho_F} \cdot \left(\sqrt{1 + \frac{1}{9} \cdot \sqrt{Ar}} - 1 \right)^2 \tag{41}$$

with:
$$Ar = \frac{d_{S,50}^3 \cdot g}{\eta_F^2} \cdot \rho_F \cdot (\rho_P - \rho_F) = \text{Archimedes-number}[-]$$
 (42)

For the turbulent area (500 < Re_P < $2 \cdot 10^5$), the Newtonian range:

$$w_{Te} = 1.74 \cdot \left(g \cdot d_{S,50} \cdot \frac{\rho_P - \rho_F}{\rho_F} \right)^{0.5} \tag{43}$$

The ranges of validity are calculated using the particle Reynolds number Re_P :

$$Re_P = \frac{w_{Te} \cdot d_{S,50} \cdot \rho_F}{\eta_F} \tag{44}$$

The following parameters are required to calculate the particle settling velocity:

- Average particle diameter [mm]
- Particle density (it is not the bulk density), it can also be equated with the bulk density [kg/m³]
- Air temperature [°C]
- Air pressure [bar(g)]

The particle settling velocity is calculated in the module for all three ranges. The Renumber test is then carried out. All values are displayed. The settling velocity for the valid Reynolds range is shown separately below.

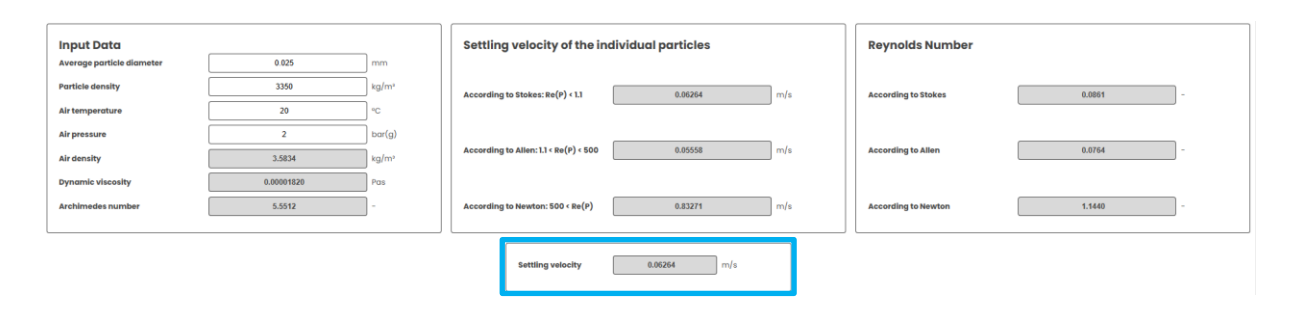


Bild 34: Module: Particle settling velocity

6.5 Fluidizing / Loosening velocity

If the pressure loss of the vertically fluidized bed remains constant above a critical gas velocity, this limiting velocity is referred to as the loosening velocity. From the so-called loosening point and over the entire fluidised bed area, the bed weight is carried by the applied pressure difference. The velocity at the loosening point is calculated as follows:

$$v_{F,L} = 42.9 \cdot \frac{1 - \varepsilon_L}{d_{S,SD}^*} \cdot \frac{\eta_F}{\varrho_F} \cdot \left(\sqrt{1 + \frac{g}{3214} \cdot \frac{\varepsilon_L^3}{(1 - \varepsilon_L)^2} \cdot (d_{S,SD}^*)^3 \cdot \frac{(\varrho_P - \varrho_F) \cdot \varrho_F}{\eta_F^2}} - 1 \right) \tag{45}$$

Die Eingabedaten zeigt Bild 37. Aus den Eingabedaten zum Gas wird die dynamische Viskosität bestimmt. Aus Schütt- und Partikeldichte wird die Porosität berechnet.





Bild 35: Module: Fluidization velocity

6.6 Rotary valve dimensioning acc. ISO 3922

ISO 3922 specifies dimensions for nine rotary valve sizes. The ISO is not a standard that is used by rotary valve suppliers. As a rule, the rotary valves from the rotary valve suppliers available on the market have dimensions and rotor volumes that deviate from the ISO. However, the ISO specifies the typical sizes. Each size has been assigned a rotor volume (Fig. 36). If you use this calculation module, you must compare the rotor volume with the finally selected rotary valve supplier.

Rotor diameter [mm]	Clear rotor width [mm]	Rotor volume [m²]	Rotational speed [1/min]	Rotor peripheral speed [m/s]	Leakage flow [Nm³/h]
160	160	0.0023	214.6	1.80	109
200	200	0.0044	109.9	1.15	118
250	250	0.0086	56.3	0.74	148
315	315	0.0172	28.1	0.46	197
400	400	0.0352	13.7	0.29	246
500	500	0.0687	7.0	0.18	301
630	630	0.1374	3.5	0.12	356
800	800	0.2813	1.7	0.07	498
1000	1000	0.5495	0.9	0.05	698

Bild 36: Sizes and technical data of rotary valves acc. ISO 3922

The programme uses the bulk density $\rho_{S'}$, the mass flow \dot{M}_{S} and the filling degree to calculate the theoretical volume flow $\dot{V}_{ZRS,S}$ that must be conveyed through the rotary valve:

$$\dot{V}_{ZRS,S} = \frac{100\%}{\text{Filling degree}} \cdot \frac{\dot{M}_S}{3,6 \cdot \rho_S} \tag{46}$$

In practice, the filling degree of an airlock / rotary feeder / Rotary valve is 100 %. However, the term "filling degree" has become established on the market. However, this usually refers to the reduction of the feed density by this factor. A cell is filled to

100%, the bulk material flowing into the cell is loosened and is not present with the bulk density, but with a reduced bulk density, also called feed density. In rotary valves for pneumatic transport, this inlet density is further reduced by the leakage air. The finer and lighter a bulk material is and the greater the pressure difference at the rotary valve, and therefore the greater the amount of leakage air flowing towards the incoming bulk material, the lower the inlet density will be. However, this is then described as the filling degree. The programme contains an equation for the filling level as a function of the bulk density and the pressure difference. Influencing variables such as feed conditions, rotary valve geometry, rotor speed, etc. are not taken into account. This value therefore serves as an initial guide. Final consultation with the rotary valve supplier is also necessary here. Figure 39 shows the course of the filling level with the stored equation as a function of the bulk density and the pressure difference.

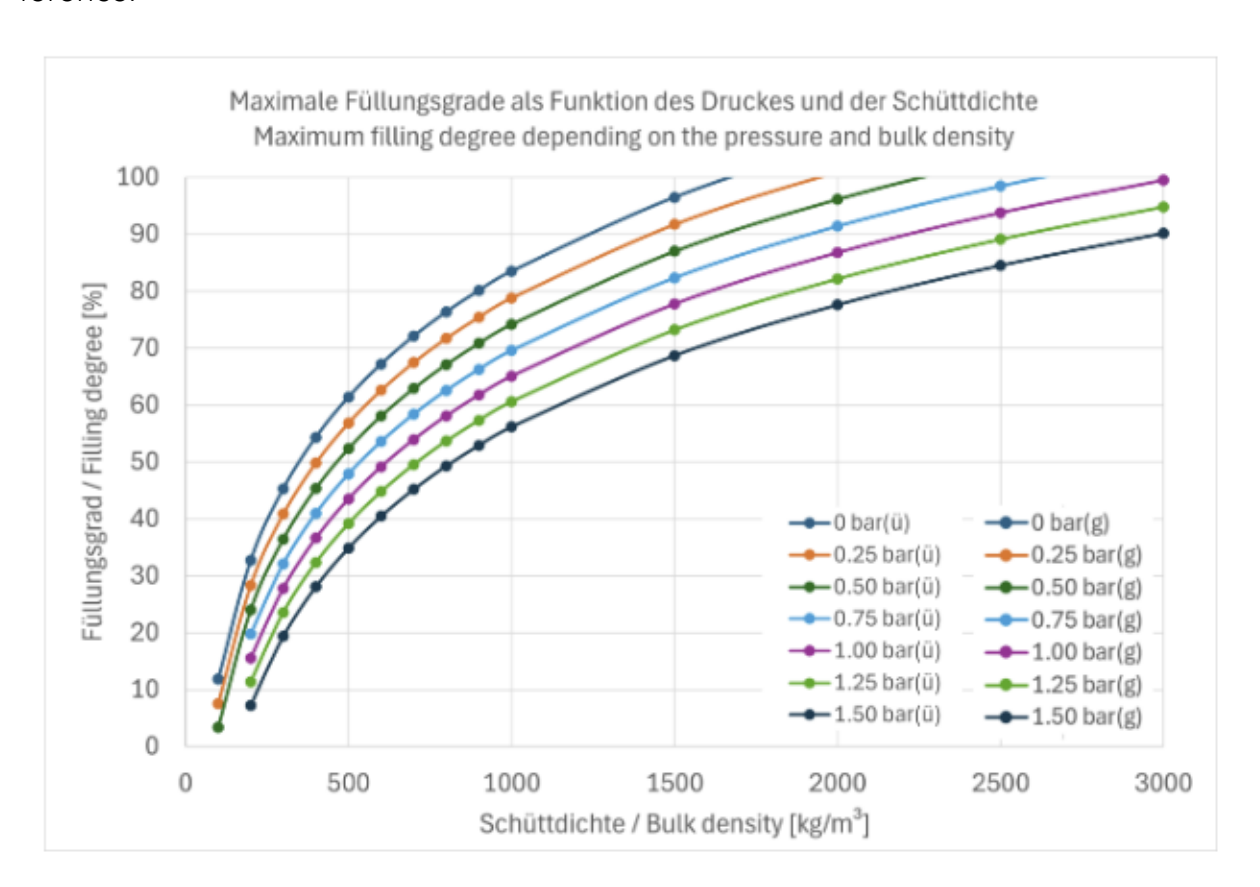


Bild 37: Filling degree of rotary feeders for fine bulk solids as a function of bulk density and pressure difference

The rotational speed of the rotary valve is determined by the rotor volume and the theoretical volume flow of the bulk material:

$$n_{ZRS} = \frac{\dot{V}_{ZRS,S} \cdot 60}{rotor \, volume} \tag{47}$$

The leakage gas volume is specified in Nm³/h. It is highly dependent on the design of the rotary valve. The values listed in the table refer to a gap of 0.2 mm between the rotor and housing during operation.



During operation, the gap is determined by the temperature of the bulk material. The warmer the bulk material is during operation, the more the rotor expands. It usually takes on the temperature of the bulk material within minutes. The housing also heats up, but not as much as the rotor, as the housing can radiate the heat to the environment. The gap during operation must therefore be defined taking into account the maximum temperature of the bulk material. The leakage gas volume refers to a closed rotor design (Fig. 40 left). If an open rotor is used in blow-through airlocks, the leakage air volume must be increased by 50 % as a first approximation. The exact leakage air quantities can be obtained from the rotary valve supplier.





Bild 38: Photo of an open (right) and closed rotor (left)

The following additional notes are listed in the programme:

- For ATEX applications, the max. peripheral speed must be limited to ≤ 1.0 m/s.
- If the falling height of the bulk material in front of the rotary feeder is > 1 m, the filling degree must be reduced. The falling of the bulk solids reduces the feed density and therefore also the filling degree.
- If the bulk material has a very good/long air retention time, the filling degree must be reduced. The leakage air flowing towards the bulk solids loosens up the bulk solids. With fine bulk solids (Geldart group A & C), the influence must be taken into account.
- A rotary feeder as a feeding device into the pneumatic conveying line directly under a silo can lead to strong pulsations, as the leakage air is not discharged evenly. It can build up in the inlet as it cannot flow out through the bulk solids column. In the case of coarse bulk solids (Geldart group D), the leakage air can flow out unhindered through the material above. The finer the bulk solids, the more resistance the air will encounter.

- Leakage air must be separated from the inlet bulk material flow for fine bulk materials (Geldart group A & C). We recommend the installation of leakage air collectors to separate the leakage air from the inlet. Although it is not possible to remove 100 % of the leakage air with leakage air collectors, a leakage air collector increases the inlet density considerably.
- A slight negative pressure of -1 ... 3 mbar in the dedusting line is recommended. The leakage air collector should be kept at a slight negative pressure to ensure that sufficient filter capacity is available.
- The wear protection of the airlock must be adapted to the pressure difference and the abrasive behaviour of the bulk material.

6.7 Pressure loss of air pipes acc. VDI-Wärmeatlas

This module calculates the pressure loss of horizontal air ducts and 90° bends. The input data (Fig. 41) is used to calculate the operational conveying gas velocity and gas density. In addition to the design data (pipe diameter and pipe roughness), they are the relevant calculation parameters for the single-phase flow. The volume flow is entered in standard conditions. The roughness is selected from Table 4, which is stored in the programme, on the basis of the selected material (blue marking in Fig. 39).

Material	Roughness K (mm)
Bitumen-coated cast iron pipe, new	0.15
Cast iron pipe, new	0.26
Cast iron pipe, rusted	4
Cast iron pipe, slightly rusted	1.5
Concrete pipe, smooth plaster	0.3
Concrete pipe, rough	1.2
Copper pipe, drawn	0.0015
Galvanized steel sheet, normal galvanized	0.15
Galvanized steel sheet, smooth (ventilation pipe)	0.07
Lead pipe, drawn	0.0015
Masonry with standard joints	1.3
Messing pipe, drawn	0.0015
Plastic pipe	0.0015
Planed boards	0.2
Riveted steel pipe	0.9
Rough boards	0.7
Seam-welded steel pipe, evenly rusted	0.4
Seam-welded steel pipe, lightly rusted	1.5
Seam-welded steel pipe, new	0.1
Seam-welded steel pipe, used and cleaned	0.2
Seam-welded steel pipe, heavily rusted	4
Seam-welded steel pipe, new, bitumen-coated	0.02
Seamless steel pipe, cleaned after long use	0.2
Seamless steel pipe, moderately rusted or lightly encrusted	0.4
Seamless steel pipe, heavily encrusted	3
Seamless steel pipe, new	0.04

Tabelle 4: Absolute roughness K for different materials in [mm]

6.7.1 Pressure loss of a "10 m section"

The pressure loss is determined iteratively from the back pressure and the air temperature according to equation (8):

$$dp_F = \lambda_F \cdot \frac{\rho_F}{2} \cdot v_F^2 \cdot \frac{L_R}{d_R} \tag{8}$$

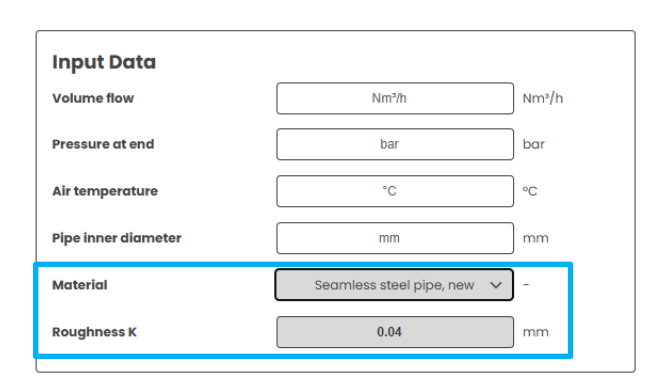


Bild 39: Input data

The pipe friction coefficient of the air λ_F is determined once for the laminar pipe flow (Re < 2320) and once for the turbulent pipe flow (Re > 2320).

Re < 2320:
$$\lambda_F = \frac{64}{Re}$$
 (48)

Re > 2320:
$$\lambda_F = \left(\frac{1}{2 \cdot \lg(\frac{d_R}{K}) + 1,14}\right)^2$$
 (49)

Whether the laminar or turbulent approach is valid is indicated by the red and green cells, Figure 40. In the upper area the laminar flow is calculated, in the lower cells the turbulent flow. When the cells are red, this flow is not valid. In the example of Fig. 40 the flow is turbulent.

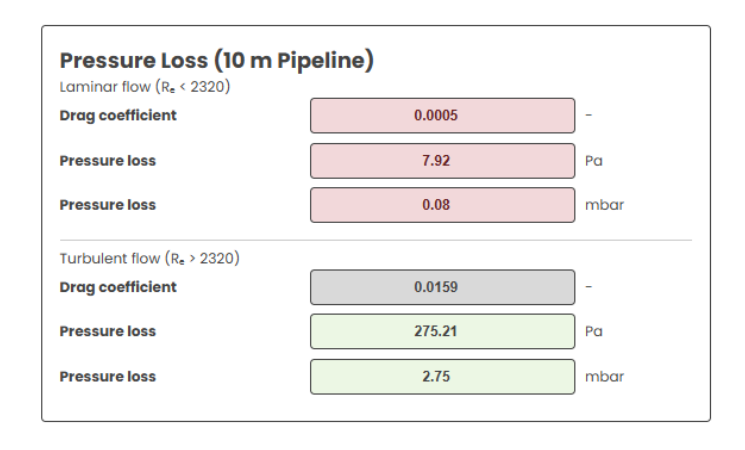


Bild 40: Calculation result for laminar and turbulent flow

As a rule of thumb for calculating the pressure loss of air ducts, equation (50) can be used:

$$dp_F = 0.02 \cdot \frac{\overline{\rho_F}}{2} \cdot v_F^2 \cdot \frac{L_R}{d_R} \tag{50}$$

L_R can be increased by 5 m per sheet.

6.7.2 Pressure loss of a 90° bend

There is no generally valid approach for calculating the pressure loss of a 90° elbow in the VDI Heat Atlas / Wärmeatlas. The material-independent resistance coefficient of a 90° elbow is selected as a function of the r/d ratio for Re $> 10^5$ (Fig. 41). This calculation method is sufficiently accurate for air ducts in pneumatic conveying systems. It can be seen that the pressure loss of a bend with the narrowest r/d ratio of 1 at is smaller than the pressure loss of a 1 - 5 m horizontal pipe.



Bild 41: Calculation result of a 90° bend

6.8 Geldart-Diagram (in progress)

Geldart [8] has developed a classification system based on his own and third-party measurements that divides dry bulk solids into four groups with regard to their fluidisation behaviour in gas/solid fluidised beds:

- A (aeratable),
- B (bubbles),
- C (cohesive),
- D.

The difference between the particle density and the gas density is plotted on the ordinate, and a characteristic particle diameter is plotted on the abscissa, in the original paper $d_{S,SD}$, here simplified and with sufficient accuracy $d_{S,5D}$.

The following properties are assigned to the four groups:

GELDART GROUP D

- Large and / or very heavy particles.
- High gas velocity in the fluidised bed.
- Gas bubble velocity is lower than interstitial gas velocity.
- Partial formation of so-called "spouded beds".
- Poor mixing behaviour, possible segregation of particles.

GELDART GROUP B

- Bubble formation begins with the onset of fluidisation.
- Slight expansion of the fluidised bed.
- After the fluidising air is switched off, the fluidised bed collapses very quickly.
- Gas bubbles rise significantly faster than the interstitial gas.
- No upper limit for bubble growth.

GELDART GROUP A

- Fine-grained particles and / or low particle density.
- Strong interparticle forces.
- Bubble size in a fluidised bed is relatively small.
- After fluidisation is switched off, the fluidised bed collapses very slowly.
- Gas bubble velocity is higher than interstitial gas velocity.

GELDART GROUP C

- High interparticle forces.
- Difficult to fluidise.
- Bed is lifted like a piston in a cylinder.
- Rat hole formation (individual free channels reaching up to the bed surface.
- Fluidisation can usually only be forced by using mechanical stirrers.

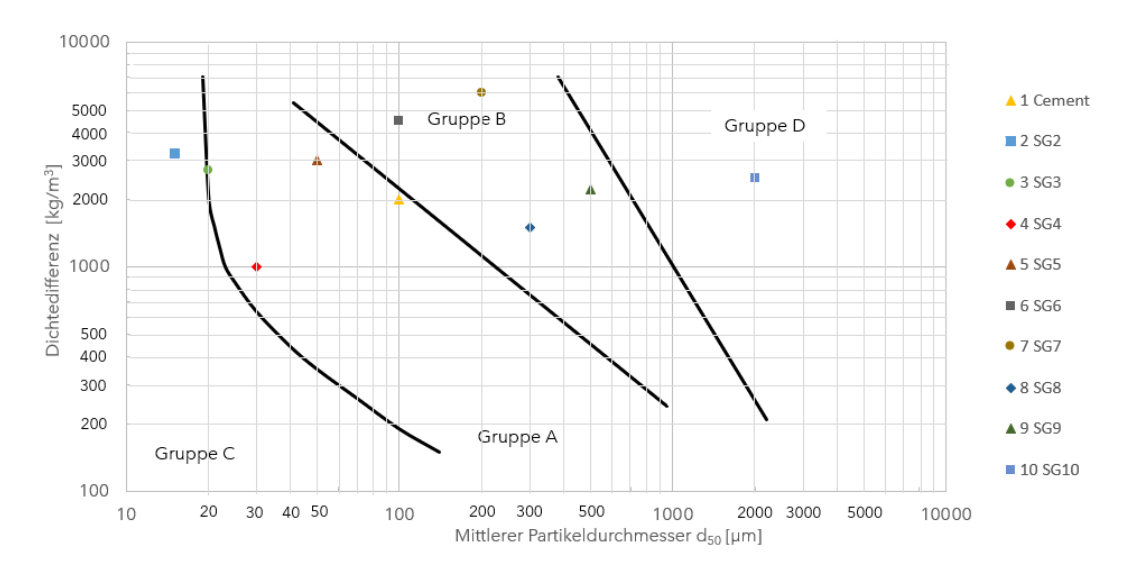


Bild 42: Geldart-Diagram with examples of bulk solids

The grey fields must be filled in to position the corresponding marker in the diagram. Up to 10 bulk materials can be displayed in the diagram at the same time.

7 List of symbols

Latin characters

Symbol	Unit	Designation
Ar	[-]	Archimedes-Number
A_R	$[m^2]$	Pipe cross section
c_{SL}	[-]	Slip factor
$d_{\scriptscriptstyle S}$	[m]	Particle diameter
$d_{S,50}$	[m]	Average particle diameter
$d_{S,SD}^{st}$	[m]	Sauter-diameter
d_R	[m]	Pipe diameter
g	$[m/s^2]$	Gravitational force
H_R	[m]	Height, altitude
L_R	[m]	Pipe section length
ṁ	[kg/s]	Mass flow
n_{ZRS}	[1/min]	Rotary valve speed
p	[N/m ²]	Pressure
T	[K],[°C]	Temperature
v_F	[m/s]	Fluid velocity (Leerrohrgeschwindigkeit)
v_S	[m/s]	Bulk material velocity, particle velocity
\dot{V}	[m ³ /s]	Volume flow
w_{Tr}	[m/s]	Settling velocity of the single particle

Greek characters

Symbol	Unit	Designation
α	[K ⁻¹]	Coefficient of linear expansion
Δ	[-]	Difference
ε	[-]	Volume fraction
$oldsymbol{\mathcal{E}}_{ extsf{F}}$	[-]	Volume fraction of the fluid
& S	[-]	Volume fraction of the bulk material
ηF	[Pas, kg/(m·s)]	Dynamic viscosity of the fluid
λ_F	[-]	Pipe drag coefficient
λ_{fi}	[-]	Drag coefficient of a single fitting
μ	[-]	Solid loading ration
ρ	[kg/m³]	Density

 $\begin{array}{ll} \rho_{\rm F} & [{\rm kg/m^3}] & {\rm Fluid~density} \\ \rho_{\rm P} & [{\rm kg/m^3}] & {\rm Particle~density} \\ \rho_{\rm S} & [{\rm kg/m^3}] & {\rm Bulk~density} \end{array}$

Indices

Symbol Designation ас Acceleration beBend F Fluid Fitting fi Total ges horizontal hoFlowing into the balance area in Flowing out of the balance room outSolid S total to vertical ve

8 Literature

- [1] Muschelknautz, E., Krambrock, W.: Vereinfachte Berechnung horizontaler pneumatischer Förderleitungen bei hoher Gutbeladung. Chemie Ingenieur Technik 41, 1164/72, Jahr 1969
- [2] Siegel, W.: Pneumatische Förderung. Würzburg, Vogel Verlag, 1991
- [3] Stegmaier, W.: fördern + heben. 28/5,6, S.363 366, 1978
- [4] Marcus, R.D.; Rizk, F.; Meijers, S.J.: Solids handling. In: Ullmann's Encyclopedia of industrial chemistry, 7. Aufl, Wiley-VCH, Weinheim (2002)
- [5] Hilgraf, P.: Pneumatische Förderung. Springer, Berlin (2019)
- [6] Weber, M.: Strömungsfördertechnik. Krausskopf-Verlag (1973)
- [7] Dhodapkar, S. V.; Klinzing, G. E.: Pressure fluctuations in pneumatic conveying systems. Powder Technology 74/2 (1993), 179-195
- [8] Blasius, H.: Das Ähnlichkeitsgesetz bei Reibungsvorgängen in Flüssigkeiten. Forschungsarbeiten des VDI, Heft 131 (1913)
- [9] Moody L.F.: Friction factors of pipe flow. Trans Am Soc Mech Eng 66 (1944), S. 671-684
- [10] Stegmaier, W.: Zur Berechnung der horizontalen pneumatischen Förderung feinkörniger Feststoffe. F+h-fördern und heben 28, Nr. 5/6 (1978), S.363-366
- [11] Sharma, A.; Mallick, S.S.: Modelling pressure drop in bends for pneumatic conveying of fine powders. Powder Technology 356 (2019), S.273-283
- [12] Mason, D.J.; Levy, A.; Marjanovic, P.: The influence of bends on the performance of pneumatic conveying systems. Advanced Powder Technology Vol.9/3 (1998), S.197-206
- [13] Bohnet, M.: Fortschritte bei der Auslegung pneumatischer Förderanlagen. Chem.-Ing.-Tech. 55/7 (1983), S.524-539
- [14] Sharma, K.; Mallick, S.S.; Mittal, A.; Wypych, P.: Modelling solids friction for fluidized dense-phase pneumatic conveying. Particulate science and technology, Vol. 20/4 (2020), S.391-403
- [15] Setia, G.; Mallick, S.S.; Pan, R.; Wypych, P.: Modelling solids friction factor for fluidized dense-phase pneumatic transport of powders using two layer flow theory. Powder Technology 294 (2016), S.80-92
- [16] Molerus, O.: Zur Beschreibung feststoffbeladener Strömungen. Chem.-Ing.Tech. 49/12 (1977), S. 945-955
- [17] Siegel, W.: Experimentelle Untersuchungen zur pneumatischen Förderung körniger Stoffe in waagerechten Rohren und Überprüfung der Ähnlichkeitsgesetze. VDI-Forschungsheft 538. Düsseldorf: VDI-Verlag (1970)



- [18] Jones, M.G.; Williams, K.C.: Solids Friction Factors for Fluidized Dense-Phase Conveying. Particulate Science and Technology 21 (2003), S.45-56
- [19] Chamber, A.J.; Marcus, R.D.: Pneumatic conveying calculations, Proceedings of 2nd International Conference on Bulk Materials Storage. Handling and transportation, Wollongong Australia (1968), S.49-52
- [20] Westmann, M.A.; Michaelidis, E.E.; Thomson, F.M.: Pressure losses due to bends in pneumatic conveying. J.Pipelines 7 (1987), S.15-20
- [21] Pan, R.: Improving Scale-up Procedures for the Design of Pneumatic Conveying Systems (1992)
- [22] Pan, R.; Wypych, P.W.: Dilute and dense phase pneumatic conveying of fly ash.Proc.6th Int. Con. Bulk Mater, Storage Transp. Wollongong Australia (1998), S.183-189
- [23] He, C.; Chen, X.; Wang, J.; Ni, H.; Xu, Y.; Zhou, H.; Xiong, Y.; Shen, X.; Chunhui, H.; Xianmei, C.; Jianhao, W.; Hongliang, N.; Yupeng, X.; Haijun, Z.; Yuanquan, X.; Xianglin, S.: Conveying characteristics and resistance characteristics in dense phase pneumatic conveying of rice husk and blendings of rice husk and coal at high pressure. Powder Technol. 227 (2012), S.51-60
- [24] Cai, L.; Liu, S.; Pan, X.; Guiling, X.; Gaoyang, Y.; Xiaoping, C.; Changsui, Z.: Comparison of Pressure drops through different bends in dense-phase pneumatic conveying system at high pressure. Exp.Thermal Fluid Sci. 57 (2014), S. 11-19
- [25] Papai, L.: Pneumatic grain conveying. Hungarian Bulletin Nr. XII/I-4 of the department VI. Hungarian Academy of Science Budapest (1954)
- [26] Vollheim, R.: Der pneumatische Transport staubförmiger Güter in senkrechten Rohrleitungen in Verbindung mit Einschleusung durch Wirbelschichten. Maschinenbautechnik 6/5 (1967), S. 237-241
- [27] Schuchart, P.: Widerstandsgesetze für den Feststofftransport in geraden Rohren und Rohrkrümmern. Dissertation Technische Universität Berlin (1968)
- [28] Siegel, W.: Berechnung von pneumatischen Saug- und Druckförderanlagen. Fördern und Heben 33 (1983), Nr. 10 S.737-740, Nr. 11 S. 817-822
- [29] Vogt, E.G.; White, R.R.: Friction in the flow of suspension. Ind.Engng.Chem. 40/9 (1948), S. 1731-1738
- [30] Hitchcock, J.A.; Jones. C.: The pneumatic conveying of spheres through straight pipes. British Journal of applied Physics 9/6 (1958), S. 218-222
- [31] Weber, M.: Grundlagen der hydraulischen und pneumatischen Rohrförderung. VDI-Bericht 371, Transrohr 80 VDI Verlag Düsseldorf (1980), S. 23-29
- [32] Siegel, W.: Pneumatische Förderung. Vogel Buchverlag (1991)



- [33] Weber, M.: Correlation analysis in the design of pneumatic transport plant. Bulk solids handling 2 (1982), S.231-233
- [34] Werner, D.: Einfluss der Korngrößenverteilung bei der pneumatischen Dichtstromförderung in vertikalen und horizontalen Rohren. Dissertation TH Karlsruhe (1982)
- [35] Gasterstädt, J.: Die experimentellen Untersuchungen des pneumatischen Fördervorganges. VDI-Forschungsheft 265 (1924)
- [36] Capes, C.E.; Nakamura, K.: Vertical Pneumatic Conveying: An Experimental Study with Particles in the Intermediate and Turbulent Flow Regimes. The Canadian Journal of Chemical Engineering 51 (1973), S.31-38
- [37] Yang, W.-C.: Correlations for Solid Friction Factors in Vertical and horizontal Pneumatic Conveyings. AIChE 20/3 (1974), S.605-607
- [38] Patro, P., Dash, S., K.: Two-fluid modelling of turbulent particle-gas suspensions in vertical pipes. Powder Technology 264 (2014). S.320-331
- [39] Plasynski, S., I., Klinzing, E.G.: High-pressure vertical pneumatic transport investigation. Powder Technology 79 (1994), S.95-109
- [40] Kerker, L.: Druckverlust und Partikelgeschwindigkeit bei der vertikalen Gas-Feststoffströmung. Verfahrenstechnik 11/9 (1977), S.549-557
- [41] Stegmaier, W.; Weber, M.: Untersuchungen zur pneumatischen Dichtstromförderung in horizontalen und vertikalen Rohren. Verfahrenstechnik 12/12 (1978), S.794-799
- [42] Zenz, F. A., Othmer, F.D.: Fluidization and Fluid-Particle Systems. Reinhold chemical Engineering Series (1960)
- [43] Muschelknautz, E.: Theoretische und experimentelle Untersuchungen über die Druckverluste pneumatischer Förderleitungen unter besonderer Berücksichtigung des Einflusses von Gutreibung und Gutgewicht. VDI 476 (1959)
- [44] https://www.youtube.com/watch?v=48VxWo_qpMA
- [45] Jenike AW (1964) Storage and flow of solids. Bull. No. 123, Engng. Exp. Station, Univ. Utah, Salt Lake City
- [46] Hilgraf, P.: Auslegung pneumatischer Dichtstromförderung auf der Grundlage von Förderversuchen Untersuchungen zum Scale-up. ZKG 42/11, Bauverlag, 1991.
- [47] Geldart, D.: Types of gas fluidization. Powder Technology 7, S.285-292, 1973